Minimax Quasi-Bayesian estimation in sparse canonical correlation analysis via a Rayleigh quotient function

Qiuyun Zhu*1 and Yves Atchade†1

¹Department of Mathematics and Statistics, Boston University

Abstract

Canonical correlation analysis (CCA) is a popular statistical technique for exploring the relationship between datasets. The estimation of sparse canonical correlation vectors has emerged in recent years as an important but challenging variation of the CCA problem, with widespread applications. Currently available rate-optimal estimators for sparse canonical correlation vectors are expensive to compute. We propose a quasi-Bayesian estimation procedure that achieves the minimax estimation rate, and yet is easy to compute by Markov Chain Monte Carlo (MCMC). The method builds on ([37]) and uses a re-scaled Rayleigh quotient function as a quasi-log-likelihood. However unlike these authors, we adopt a Bayesian framework that combines this quasi-log-likelihood with a spike-and-slab prior that serves to regularize the inference and promote sparsity. We investigated the empirical behavior of the proposed method on both continuous and truncated data, and we noted that it outperforms several state-of-the-art methods. As an application, we use the methodology to maximally correlate clinical variables and proteomic data for a better understanding of covid-19 disease.

1 Introduction

Canonical correlation analysis is a statistical technique –dating back at least to [18] – that is used to maximally correlate multiple datasets for joint analysis. The technique has become a fundamental tool in biomedical research where technological advances have made it possible to observe fundamental biological phenomena from multiple viewpoints, the so-called multi-omic datasets ([42]; [26]; [29]). Over the past two decades, limited sample sizes, growing dimensionality, and the search for meaningful biological interpretations, have led to the development of sparse canonical correlation analysis ([41, 42, 28, 40, 17]), where a sparsity assumption is imposed on the canonical correlation vectors.

Statistically optimal estimation of sparse CCA has been considered in several works. ([13]) derived the minimax rate of estimation of sparse CCA, and proposed a two-stage estimation procedure that achieves the rate. ([37]) uses a generalized Rayleigh quotient approach to propose a two-stage estimator that also achieves the minimax rate. The main limitation of these rate-optimal estimation procedures is their high computational cost. Specifically, in both approaches,

^{*}rachyun@bu.edu

[†]atchade@bu.edu

each iteration of the first-stage optimization problem has a computational cost of $O(p^3)$, where p is the joint number of variables in the datasets. Furthermore, the two-stage nature of these estimators can also be a problem in practice, since it can be hard to set the required stopping criterion of the first-stage solver that guarantees a good behavior of the final estimator.

We address these issues by proposing in this paper a conceptually simple, yet rate-optimal quasi-Bayesian estimator for sparse CCA. More specifically, building on ([37]), we propose a quasi-Bayesian or (PAC-Bayesian) approach that employs a re-scaled version of the Rayleigh quotient function as a quasi-log-likelihood function together with a spike and slab prior to obtain a quasi-posterior distribution. Our sparse CCA estimator is then defined as a posterior mean of the quasi-posterior distribution. The method is agnostic to the covariance matrix estimators used in constructing the Rayleigh quotient function. For example, we observe in our experiments that both the sample covariance matrix estimator and the Kendall's-tau-based covariance matrix estimator ([43]) work well, even when they are singular. In fact, although we do not pursue this here, one can straightforwardly extend our method to solve other generalized eigenvalue problems in the same spirit as [37].

We analyze the proposed estimator and derive its convergence rate (see Theorem 4). In the particular case where sample covariance matrices are used to estimate the Rayleigh quotient, we show that the estimator achieves the minimax rate for sparse CCA estimation, under some modest sample size condition.

The idea of using a Bayesian framework to produce frequentist estimators is of course well-known in statistical decision theory. The extension of the idea to allow for pseudo-likelihood functions is more recent in the statistics and econometrics literature ([10]), but has a longer history in machine learning under the name of PAC-Bayesian learning ([23, 9]).

We propose a Markov Chain Monte Carlo algorithm based on simulated tempering to sample from the quasi-posterior distribution, and compute the estimator. In stationarity, the proposed algorithm has a per-iteration cost of $O(s_{\star}^2p)$, where s_{\star} is the true sparsity level of the signal. Furthermore, we show empirically that for sufficiently large sample size, the mixing time of the algorithm scales linearly in p. Overall, our estimator has a more favorable computational cost than the Rifle estimator of ([37]).

The remaining of the paper is organized as follows. In Section 2 we introduce our estimation procedure and derive its convergence rate. In Section 3 we detail a simulated tempering algorithm to sample from the resulting quasi-posterior distribution. In Section 4, we study the numerical behavior of the proposed method on both continuous and truncated data, and compare it with other methods. In Section 5, we apply the method in a real data analysis that aims to correlate clinical and proteomic data from covid-19 patients, for a better understanding of the disease. Our analysis identifies Alpha-1-acid glycoprotein 1 (AGP 1) as playing an important role in the progression of Covid-19 into a severe illness.

2 Quasi-Bayesian sparse canonical correlation analysis using a Rayleigh quotient function

Let $(X,Y) \in \mathbb{R}^{p_x} \times \mathbb{R}^{p_y}$ be a pair of high-dimensional zero-mean random vectors with joint distribution f, with covariance matrices $\Sigma_x \stackrel{\text{def}}{=} \mathbb{E}(XX^{\mathrm{T}})$, $\Sigma_y \stackrel{\text{def}}{=} \mathbb{E}(YY^{\mathrm{T}})$ and $\Sigma_{xy} \stackrel{\text{def}}{=} \mathbb{E}(XY^{\mathrm{T}})$. Let $(v_{x\star}, v_{y\star}) \in \mathbb{R}^{p_x} \times \mathbb{R}^{p_y}$ be a pair of principal canonical correlation vectors for f. That is, the vector $(v_{x\star}, v_{y\star}) \in \mathbb{R}^{p_x} \times \mathbb{R}^{p_y}$ solves the following optimization problem:

$$\max_{v_x \in \mathbb{R}^{p_x}, \ v_y \in \mathbb{R}^{p_y}} v_x^T \Sigma_{xy} v_y \quad \text{s.t.} \quad v_x^T \Sigma_x v_x = v_y^T \Sigma_y v_y = 1.$$
 (1)

It what follows we set $\theta_{\star} \stackrel{\text{def}}{=} (v_{x\star}^{\text{T}}, v_{y\star}^{\text{T}})^{\text{T}}$ which is our main parameter of interest. Without any loss of generality we assume that $\|\theta_{\star}\|_2 = 1$. Clearly, θ_{\star} is estimable only up to a sign. If we set $p \stackrel{\text{def}}{=} p_x + p_y$, and define the matrices

$$A \stackrel{\text{def}}{=} \begin{bmatrix} 0 & \Sigma_{xy} \\ \Sigma_{xy}^{\text{T}} & 0 \end{bmatrix}, \qquad B \stackrel{\text{def}}{=} \begin{bmatrix} \Sigma_x & 0 \\ 0 & \Sigma_y \end{bmatrix}, \quad \text{and} \quad \Sigma \stackrel{\text{def}}{=} A + B, \tag{2}$$

then it is easily seen that problem (1) is equivalent to the following generalized eigenvalue problem (GEP):

$$\max_{\theta = (v_x^{\mathrm{T}}, v_y^{\mathrm{T}})^{\mathrm{T}} \in \mathbb{R}^p} \theta^{\mathrm{T}} A \theta \quad \text{s.t.} \quad \theta^{\mathrm{T}} B \theta = 2.$$
 (3)

This is because $\max\{\sqrt{xy}: x \ge 0, y \ge 0, x + y = 2\}$ is achieved by taking x = y = 1. Clearly, finding a solution of (3), is equivalent to finding a solution of

$$\max_{\theta = (v_x^{\mathrm{T}}, v_y^{\mathrm{T}})^{\mathrm{T}} \in \mathbb{R}^p} \mathsf{R}(\theta) \stackrel{\text{def}}{=} \frac{\theta^{\mathrm{T}} A \theta}{\theta^{\mathrm{T}} B \theta},\tag{4}$$

where we convene that 0/0 = 0. The objective function R in (4) is known as the *(generalized)* Rayleigh quotient of A and B. To the best of our knowledge the idea of estimating the sparse canonical correlation vectors by directly targeting the Rayleigh quotient was first developed by ([37]). Note that solving (4) in practice requires specifying matrices A and B, which are typically unknown. In practice, one often constructs estimators of A and B, denoted by \hat{A} and \hat{B} , respectively, based on n i.i.d. samples $\mathbf{Z} \stackrel{\text{def}}{=} \{(X_1, Y_1), \dots, (X_n, Y_n)\}$ from f. Specifically, given \mathbf{Z} , one first constructs estimators of Σ_x , Σ_y , and Σ_{xy} , denoted by $\hat{\Sigma}_x$, $\hat{\Sigma}_y$, and $\hat{\Sigma}_{xy}$, respectively, and then constructs \hat{A} and \hat{B} from $\hat{\Sigma}_x$, $\hat{\Sigma}_y$, and $\hat{\Sigma}_{xy}$, in the same fashion as in (2) – In Section 4, we will provide some examples of how to construct the estimators $\hat{\Sigma}_x$, $\hat{\Sigma}_y$, and $\hat{\Sigma}_{xy}$. One then replaces the Rayleigh quotient by its sample version defined as

$$\mathsf{R}_n(\theta; \mathbf{Z}) \stackrel{\mathrm{def}}{=} \frac{\theta^{\mathrm{T}} \hat{A} \theta}{\theta^{\mathrm{T}} \hat{B} \theta}, \ \theta \in \mathbb{R}^{p_x + p_y}.$$

It is worth mentioning that in the high-dimensional regime, direct maximization of R_n poses problems (the constructed estimators $\hat{\Sigma}_x$ and $\hat{\Sigma}_y$, e.g. sample covariance matrices, are usually singular, and inconsistent). [37] addressed these issues by maximixing $R_n(\cdot; \mathbf{Z})$ under a sparsity contraint. The authors show that this maximization problem can be solved provided that a good initial value is provided. However, finding a good initial value is very costly. Furthermore, given that the Rayleigh quotient typically admits several local maxima (and possibly minima), and given the need to encode a prior sparsity information, we argue that a Bayesian framework is a more effective approach for leveraging the Rayleigh quotient for sparse CCA.

2.1 A Quasi-Bayesian approach

We propose to use the quasi-Bayesian framework to turn the Rayleigh quotient CCA estimator of ([37]) into a Bayesian procedure. More precisely, we shall infer θ_{\star} by using the function

$$\theta \mapsto n\mathsf{R}_n(\theta; \mathbf{Z})$$
 (5)

as a log-likelihood in a Bayesian inference for θ_{\star} . For the prior distribution on θ , we choose the spike-and-slab distribution, a common choice for Bayesian sparse modeling ([15]). Given a variable selection parameter $\delta \in \Delta \stackrel{\text{def}}{=} \{0,1\}^p$, let the conditional distribution of θ given δ be

$$\pi(\theta|\delta) = \prod_{j=1}^{p} \pi(\theta_j|\delta), \quad \text{where} \quad \theta_j|\delta = \theta_j|\delta_j \sim \begin{cases} \mathbf{N}(0, \rho_1^{-1}), & \text{if } \delta_j = 1\\ \mathbf{N}(0, \rho_0^{-1}), & \text{if } \delta_j = 0 \end{cases}, \tag{6}$$

and $\rho_0 > \rho_1 > 0$ are precision parameters. In addition, the prior distribution of δ is taken as an independent product of Bernoulli distributions with odd-ratio p^{-u} for some parameter u > 1, constraint to be s-sparse, for some sparsity parameter $1 \le s \le p$:

$$\pi(\delta) \propto \left(\frac{1}{p^{\mathsf{u}}}\right)^{\|\delta\|_0} \mathbf{1}_{\Delta_s}(\delta), \quad \text{where} \quad \Delta_s \stackrel{\text{def}}{=} \{\delta \in \Delta : \|\delta\|_0 \le s\}.$$
 (7)

If we combine the spike-and-slab prior with the quasi-log-likelihood in (5), we then obtain the quasi-posterior distribution

$$\Pi(\delta, d\theta | \mathbf{Z}) \propto \mathbf{1}_{\Delta_s}(\delta) \exp\left(a\|\delta\|_0 - \frac{\rho_1}{2}\|\theta_\delta\|_2^2 - \frac{\rho_0}{2}\|\theta - \theta_\delta\|_2^2\right) \exp\left(n\mathsf{R}_n(\theta_\delta; \mathbf{Z})\right) d\theta, \tag{8}$$

where θ_{δ} is the entry-wise product of θ and δ , $\|\cdot\|_2$ the Euclidean norm, and

$$\mathsf{a} \stackrel{\mathrm{def}}{=} \log \left(\frac{1}{p^\mathsf{u}} \sqrt{\frac{\rho_1}{\rho_0}} \right).$$

Given the quasi-posterior distribution $\Pi(\cdot|\mathbf{Z})$ we propose to estimate the projector $\theta_{\star}\theta_{\star}^{\mathrm{T}}$ associated to θ_{\star} by

$$\widehat{\mathcal{P}} \stackrel{\text{def}}{=} \int_{\Delta \times \mathbb{R}^p} \frac{\theta_{\delta} \theta_{\delta}^{\mathrm{T}}}{\|\theta_{\delta}\|_{2}^{2}} \Pi(\mathrm{d}\delta, \mathrm{d}\theta | \mathbf{Z}). \tag{9}$$

The spike-and-slab prior specified in (6) and (7) is fairly standard, and goes back at least to ([15]). However the way it is combined with the pseudo-likelihood to give (8) is nonstandard, and follows ([2]). The approach can be viewed as an approximation of the point-mass spike-and-slab prior ([25]), using the pseudo-prior device of ([8]). The appealing feature of this approach is that in (8) the parameter θ enters the likelihood only through its sparsified form θ_{δ} . This has the effect of decoupling the active components (those corresponding to $\delta_j = 1$) and the non-active components, and is particularly attractive from the computational standpoint. The parameter ρ_0 – the precision parameter of the non-selected components – has no effect on the statistical recovery of the selected components of θ , but can adversely impact the MCMC mixing if a value too large is used. We suggest setting $\rho_0 = n$, in order to match the posterior variance of selected components that are actually 0. The posterior distribution Π is very robust to the choice of ρ_1 and μ_0 , and we find that choosing $\rho_1 \approx 1$, and $\mu_0 \in (1,2]$ works well. We discuss the choice of s in the next sub-section.

2.1.1 Existence of $\Pi(\cdot|\mathbf{Z})$

Clearly $\Pi(\cdot|\mathbf{Z})$ is not a posterior distribution in the standard sense, since $n\mathsf{R}_n$ is not a proper log-likelihood. As such it may not be well-defined. The next proposition gives a simple condition under which $\Pi(\cdot|\mathbf{Z})$ is well-defined.

Proposition 1. Suppose that **Z** is such that

$$\theta^{\mathrm{T}} \hat{B} \theta > 0$$
, for all $\theta \in \mathbb{R}^p$ such that $0 < \|\theta\|_0 \le s$. (10)

Then $\Pi(\cdot|\mathbf{Z})$ is a well-defined probability measure on $\Delta \times \mathbb{R}^p$.

Proof. Indeed, under the stated assumption the normalizing constant of $\Pi(\cdot|\mathbf{Z})$ is bounded from above by

$$\sum_{\delta \in \Delta_s} \pi(\delta) \int_{\mathbb{R}^p} \pi(\theta|\delta) e^{n\frac{\lambda_{\max}(\hat{A},s)}{\lambda_{\min}(\hat{B},s)}} \mathrm{d}\theta \leq e^{n\frac{\lambda_{\max}(\hat{A},s)}{\lambda_{\min}(\hat{B},s)}} < \infty,$$

where $\lambda_{\mathsf{max}}(A, s)$ (resp. $\lambda_{\mathsf{min}}(A, s)$)) denotes the largest (resp. smallest) eigenvalues of submatrices obtained by taking at most s row and columns of A (see below for precise definition). \square

Remark 2. Condition (10) is typically not stringent. For instance, if \hat{B} is formed from the sample covariance matrices of X and Y, and X and Y are sub-Gaussian random vectors, then with high probability (10) holds as soon as the sample size satisfies $n \geq Cs \log(p_x \vee p_y)$, where C is some absolute constant that depends only on Σ_x, Σ_y and the sub-Gaussian norm of X, Y.

Proposition 1 sheds light on the sparsity parameter s. Proposition 1 shows that the sparsity parameter s should be chosen such that $\lambda_{\min}(\hat{B}, s) > 0$. In view of the last remark the choice

$$s = \frac{cn}{\log(p)}$$
, for some constant $c \approx 1$

seems natural. When $s_{\star} = \|\theta_{\star}\|_0$ is much smaller than $n/\log(p)$, the MCMC sampler can actually be safely run without explicitly specifying a value for s, that is without the need to enforce the constraint $\delta \in \Delta_s$. Indeed by posterior contraction, the MCMC sampler in those cases never drift toward big models. In all our simulations we have implemented the algorithm without specifying s.

2.2 Rate of convergence

We show in this section that the quasi-Bayesian estimator $\widehat{\mathcal{P}}$ of $\theta_{\star}\theta_{\star}^{\mathrm{T}}$ introduced in (9) is rate-optimal – in a frequentist sense. For $M, N \in \mathbb{R}^{q \times q}$, for some $q \geq 1$, we define

$$\langle M,N\rangle_{\mathsf{F}} \stackrel{\mathrm{def}}{=} \mathsf{Tr}(M^{\scriptscriptstyle{\mathsf{T}}}N), \quad \|M\|_{\mathsf{F}} \stackrel{\mathrm{def}}{=} \sqrt{\langle M,M\rangle_{\mathsf{F}}}, \quad \mathrm{and} \quad \|M\|_{\mathsf{op}} \stackrel{\mathrm{def}}{=} \sup_{u \in \mathbb{R}^q: \; \|u\|_2 = 1} \; \|Mu\|_2.$$

For $J \subseteq \{1, \ldots, q\}$, $M_{J,J}$ denotes the submatrix $(M_{ij})_{i,j \in J}$. Given an integer $k \geq 1$, we set

$$\lambda_{\mathsf{min}}(M,k) \ \stackrel{\mathrm{def}}{=} \ \min_{u \in \mathbb{R}^q, \ \|u\|_2 = 1, \|u\|_0 \le k} \ u^{\scriptscriptstyle \mathrm{T}} M u, \quad \text{and} \quad \lambda_{\mathsf{max}}(M,k) \ \stackrel{\mathrm{def}}{=} \ \max_{u \in \mathbb{R}^q, \ \|u\|_2 = 1, \|u\|_0 \le k} \ u^{\scriptscriptstyle \mathrm{T}} M u.$$

Given integer $\alpha \geq 1$, we set

$$\lambda_{\max}^{(\alpha)}(M,s) \ \stackrel{\mathrm{def}}{=} \max_{\substack{J \subseteq [1:q], \ \|J\|_0 = s}} \ \max_{\substack{A \in \mathbb{R}^{s \times s}: \ \|A\|_{\mathbb{F}} = 1 \\ \mathrm{Rank}(A) \le \alpha}} \ |\langle M_{J,J}, A \rangle| \,,$$

where [1:q] is a short for $\{1,\ldots,q\}$. We note that $\lambda_{\mathsf{max}}^{(1)}(M,k) = \lambda_{\mathsf{max}}(M,k)$. We first make the following basic assumption without which the sparse CCA problem would not be well defined.

H 1. $(X^{\mathrm{T}}, Y^{\mathrm{T}}) \sim f$ with positive definite covariance matrices Σ_x , Σ_y , and Σ , and a principal canonical vector $\theta_{\star} = (v_{x\star}^{\mathrm{T}}, v_{y\star}^{\mathrm{T}})^{\mathrm{T}}$, such that $s_{\star} \stackrel{\mathrm{def}}{=} \|\theta_{\star}\|_{0} \leq s$. Furthermore, the difference between the largest and second largest eigenvalue of $S \stackrel{\mathrm{def}}{=} B^{-1/2} \Sigma B^{-1/2}$ (denoted by gap), is positive.

Our main assumption on the data generation process is the following.

H 2. $\mathbf{Z} \stackrel{\text{def}}{=} \{(X_1^{\mathrm{T}}, Y_1^{\mathrm{T}})^{\mathrm{T}}, \dots, (X_n^{\mathrm{T}}, Y_n^{\mathrm{T}})^{\mathrm{T}}\}\$ is a sequence of n i.i.d. random variables from f, and there exist absolute constants $0 < \underline{\kappa} \le \bar{\kappa}$ such that the following holds.

1.

$$\begin{split} & \min\left(\lambda_{\min}(\hat{\Sigma}_x, s + s_{\star}), \ \lambda_{\min}(\hat{\Sigma}_y, s + s_{\star}), \ \lambda_{\min}(\hat{\Sigma}, s + s_{\star})\right) \geq \underline{\kappa}, \\ & \max\left(\lambda_{\max}(\hat{\Sigma}_x, s + s_{\star}), \ \lambda_{\max}(\hat{\Sigma}_y, s + s_{\star}), \lambda_{\max}(\hat{\Sigma}, s + s_{\star}), \right) \leq \bar{\kappa}. \end{split}$$

2. For some constant r_1 (depending possibly on n, p)

$$\max\left(\lambda_{\max}^{(2)}(\hat{\Sigma}_x - \Sigma_x, s + s_\star), \ \lambda_{\max}^{(2)}(\hat{\Sigma}_y - \Sigma_y, s + s_\star), \ \lambda_{\max}^{(2)}(\hat{\Sigma} - \Sigma_x, s + s_\star)\right) \leq r_1.$$

Remark 3. We first remark that if H2 holds, then for all $\theta \in \mathbb{R}^p$, with $\|\theta\|_0 \leq s$,

$$\theta^{\mathrm{T}} \hat{B} \theta = \theta^{\mathrm{T}} \begin{pmatrix} \hat{\Sigma}_x & 0 \\ 0 & \hat{\Sigma}_y \end{pmatrix} \theta \ge \underline{\kappa} \|\theta\|_2^2.$$

Meaning that H2 implies that the quasi-posterior distribution $\Pi(\cdot|\mathbf{Z})$ is well-defined, by Proposition 1.

Theorem 4. Assume H1, and H2, and choose u > 1 such that $p^{u-1} > 2$, and $p^{u} \ge s_{\star} \exp(1)$. Set

$$\epsilon \stackrel{\text{def}}{=} \frac{r_1}{\text{gap}}.\tag{11}$$

There exists some absolute constant C_0 that depends only on $\underline{\kappa}$ and $\bar{\kappa}$, such that the following holds. For all $M > C_0$ such that

$$\frac{M^2}{8\operatorname{gap}} \left(\frac{\kappa}{\bar{\kappa}}\right)^2 n r_1^2 \ge (s_\star + 1)(\mathsf{u} + 1)\log\left(p \lor (c_0 n)\right),\tag{12}$$

where c_0 is some absolute constant that depends only on $\underline{\kappa}$ and $\bar{\kappa}$, the estimator $\widehat{\mathcal{P}}$ in (9) satisfies

$$\left\|\widehat{\mathcal{P}} - \theta_{\star}\theta_{\star}^{\mathrm{T}}\right\|_{F} \leq \int_{\Delta_{\star} \times \mathbb{R}^{p}} \left\|\frac{\theta_{\delta}\theta_{\delta}^{\mathrm{T}}}{\|\theta_{\delta}\|_{2}^{2}} - \theta_{\star}\theta_{\star}^{\mathrm{T}}\right\|_{F} \Pi\left(\mathrm{d}\delta, \mathrm{d}\theta | \mathbf{Z}\right) \leq M\epsilon + 2e^{-\frac{M^{2}}{8\mathsf{gap}}\left(\frac{\kappa}{\tilde{\kappa}}\right)^{2}nr_{1}^{2}}.$$

Proof. See Section A.
$$\Box$$

Since the term $2e^{-\frac{M^2}{8\text{gap}}(\frac{\kappa}{\hat{\kappa}})^2 n r_1^2}$ is much smaller than $M\epsilon$ (under (12)), the main conclusion of the theorem is that the posterior mean $\widehat{\mathcal{P}}$, as a frequentist estimator, estimates $\theta_{\star}\theta_{\star}^{\mathrm{T}}$ at the rate $M\epsilon$. In the particular case where $\hat{\Sigma}_x, \hat{\Sigma}_y$ and $\hat{\Sigma}$ are covariances matrices of sub-Gaussian random

vectors, we show in Proposition 5 (see below) that $\mathbf{r}_1 = C_0 \sqrt{s \log(p)/n}$, under the sample size condition $n \ge C_0 s \log(p)$. In that case the condition in (12) becomes

$$\frac{M^2}{8\mathsf{gap}} \left(\frac{\kappa}{\bar{\kappa}}\right)^2 C_0^2 s \log(p) \ge (s_\star + 1)(\mathsf{u} + 1) \log \left(p \lor (c_0 n)\right),$$

which is easily satisfied. Hence the convergence rate of the estimator is

$$\epsilon = \frac{1}{\mathsf{gap}} \sqrt{\frac{s \log(p)}{n}},\tag{13}$$

which achieves the minimax rate of the CCA problem, as derived in ([13]). Note that our result does not contradict ([14]), which conjectures that $n \geq C_0 s^2 \log(p)$ is a necessary sample size condition for estimating θ_{\star} at the rate ϵ , with a polynomial complexity estimator, because Theorem 4 does not make any claim about the computational complexity of $\widehat{\mathcal{P}}$. In practice we compute $\widehat{\mathcal{P}}$ by Markov Chain Monte Carlo, and interestingly we notice that the mixing of our proposed MCMC sampler depends on the sample size in a way that confirms the conjecture of ([14]) (see Section 4.2.).

2.2.1 On Assumption H2

It is well-known that Assumption H2-(1) holds true in the particular case of covariance matrices of sub-Gaussian random vectors, provided that the sample size satisfies $n \geq c_0 s \log(p)$, for some absolute constant c_0 . See for instance [30] Theorem 1, or [14] Lemma 6.5 for the Gaussian case, and [33] Theorem 3.2 for more general sub-Gaussian distributions. Under roughly the same sample size conditions, H2-(2) is also known to hold as we show below.

Proposition 5. Suppose that $Z_i \stackrel{\text{def}}{=} (X_i^{\mathsf{T}}, Y_i^{\mathsf{T}})^{\mathsf{T}}$ are i.i.d. random vectors from a mean-zero sub-Gaussian distribution f, with sub-Gaussian norm $K \stackrel{\text{def}}{=} \sup\{\|\langle Z, u \rangle\|_{\psi_2}, \ u \in \mathbb{R}^p, \ \|u\|_2 = 1\}$, where $\|\cdot\|_{\psi_2}$ refers to the sub-Gaussian norm of a random variable. Let $\hat{\Sigma}_x = n^{-1} \sum_{i=1}^n X_i X_i^{\mathsf{T}}$, $\hat{\Sigma}_y = n^{-1} \sum_{i=1}^n Y_i Y_i^{\mathsf{T}}$, and $\hat{\Sigma} = n^{-1} \sum_{i=1}^n Z_i Z_i^{\mathsf{T}}$. There exist an absolute constants $c_0, C > 1$, such that for $n \geq 4c_0 s \log(p)$,

$$\max\left(\lambda_{\max}^{(\alpha)}(\hat{\Sigma}_x - \Sigma_x, s), \ \lambda_{\max}^{(\alpha)}(\hat{\Sigma}_y - \Sigma_y, s), \ \lambda_{\max}^{(\alpha)}(\hat{\Sigma} - \Sigma, s)\right) \leq CK^2\lambda_{\max}(\Sigma, s)\sqrt{\frac{c_0\alpha s\log(p)}{n}},$$

with probability $1 - 2p^{-(c_0-1)s}$.

Proof. We present the details of this claim for $\hat{\Sigma}$, the argument being similar for the other two covariance matrices. For any $J \subset [1:p]$ of size s, we have

$$\|\hat{\Sigma}_{J,J} - \Sigma_{J,J}\|_{\mathsf{op}} = \|\Sigma_{J,J}^{1/2} \left(\Sigma_{J,J}^{-1/2} \hat{\Sigma}_{J,J} \Sigma_{J,J}^{-1/2} - I_s\right) \Sigma_{J,J}^{1/2}\|_{\mathsf{op}} \leq \|\Sigma_{J,J}^{1/2}\|_{\mathsf{op}}^2 \times \|\frac{1}{n} \sum_{i=1}^n U_{iJ} U_{iJ}^{\mathsf{T}} - I_s\|_{\mathsf{op}},$$

where $U_{iJ} \stackrel{\text{def}}{=} \Sigma_{J,J}^{-1/2} Z_{iJ}$, where $Z_{iJ} = (Z_{ij})_{j \in J}$, is mean zero and isotropic. By Theorem 4.6.1 (Equation 4.22) of ([38]), provided that $n \geq 4c_0 s \log(p)$ for some absolute constant $c_0 > 1$, we have

$$\|\hat{\Sigma}_{J,J} - \Sigma_{J,J}\|_{\mathsf{op}} \le CK^2 \|\Sigma_{J,J}^{1/2}\|_{\mathsf{op}}^2 \sqrt{\frac{c_0 s \log(p)}{n}},$$

with probability at least $1 - 2p^{-c_0s}$. Therefore, for any matrix $A \in \mathbb{R}^{s \times s}$, with $||A||_{\mathsf{F}} = 1$, and $\mathsf{Rank}(A) \leq \alpha$, using the singular value decomposition of A, we have

$$\max_{\substack{A \in \mathbb{R}^{s \times s}: \, \|A\|_{\mathbb{F}} = 1 \\ \operatorname{Rank}(A) \leq \alpha}} \left| \left\langle \hat{\Sigma}_{J,J} - \Sigma_{J,J}, A \right\rangle \right| \leq \sqrt{\alpha} \|\hat{\Sigma}_{J,J} - \Sigma_{J,J}\|_{\operatorname{op}} \leq CK^2 \lambda_{\max}(\Sigma, s) \sqrt{\frac{c_0 \alpha s \log(p)}{n}}.$$

Since the number of subsets of [1:p] of size s is smaller than p^s , we conclude with a union bound argument that

$$\lambda_{\max}^{(\alpha)}(\hat{\Sigma} - \Sigma, s) \le CK^2 \lambda_{\max}(\Sigma, s) \sqrt{\frac{c_0 \alpha s \log(p)}{n}},$$

with probability $1 - 2p^{-(c_0 - 1)s}$.

2.2.2 Bayesian inference

In this paper we have used the posterior mean of a quasi-posterior distribution as a frequentist estimator. The idea of using a Bayesian framework to produce a frequentist estimator is of course a very old one. In fact it is well known in classical statistical that all "good" estimators are Bayesian. The extension of the idea to allow for pseudo-likelihood functions is more recent in the statistics and econometrics literature ([10]), but the approach has a long history in machine learning under the name of PAC-Bayesian learning ([23, 9]). A natural question here is whether one can use the full quasi-posterior distirbution $\Pi(\cdot|\mathbf{Z})$ to carry inference on θ_{\star} , for instance through credible sets. The difficulty is the lack of calibration of the quasi-likelihood function (we could easily have used 2n instead n as a scaling factor in the Rayleigh quotient). These issues have been explored in the low-dimensional setting ([6, 35]), but remain largely open in the high-dimensional setting. We leave this question as a possible future research. Currently we do not advocate the use of our quasi-posterior distribution for Bayesian inference on θ_{\star} .

3 Markov Chain Monte Carlo

It is straightforward to design an MCMC sampler to sample from (8). However we face the challenge that the distribution has possibly multiple modes, with a complicated landscape. Indeed, any generalized eigenvector of (\hat{A}, \hat{B}) is a stationary points of the Rayleigh quotient $R_n(\cdot; \mathbf{Z})$. In addition, if (u, v) maximizes $R_n(\cdot; \mathbf{Z})$, so does (-u, -v). To deal with this challenge, we leverage simulated tempering (see e.g., [16]), a MCMC sampling technique that has shown promising performance in sampling from multi-modal distributions.

Given K temperatures $1 = t_1 < t_2 < \ldots < t_K$, and K positive weights c_1, \ldots, c_K , we introduce an extended distribution on $X \stackrel{\text{def}}{=} \Delta \times \mathbb{R}^p \times \{1, \ldots, K\}$, which is

$$\bar{\Pi}(\delta, d\theta, k | \mathbf{Z}) \propto \frac{1}{c_k} \exp\left(\frac{a}{t_k} \|\delta\|_0\right) \exp\left(-\frac{\rho_1}{2t_k} \|\theta_\delta\|_2^2 - \frac{\rho_0}{2t_k} \|\theta - \theta_\delta\|_2^2\right) \exp\left(\frac{n}{t_k} \mathsf{R}_n(\theta_\delta; \mathbf{Z})\right) d\theta. \quad (14)$$

We recover the distribution (8) as the conditional distribution of (δ, θ) given k = 1 in (14). To sample from (14), we use a Metropolis-within-Gibbs strategy summarized in Algorithm 1.

First, we update δ by applying a Gibbs sampler to the conditional distribution of δ given k and θ . Note that the conditional distribution of δ_j given k, θ and δ_{-j} , where $\delta_{-j} \stackrel{\text{def}}{=} (\delta_1, \dots, \delta_{j-1}, \delta_{j+1}, \dots, \delta_p)$,

Algorithm 1 Simulated tempering for sparse canonical correlation analysis

Model Input: Matrices \hat{A}, \hat{B} , prior parameters ρ_0, ρ_1, q .

MCMC Input: Number of iterations N, batch size J, temperatures $1 = t_1 < \ldots, < t_K$, weights (c_1, \ldots, c_K) , and step-sizes (η_1, \ldots, η_K) .

Initialization: Set $k^{(0)} = 1$. Draw $\delta_j^{(0)} \stackrel{i.i.d.}{\sim} \mathbf{Ber}(0.5), \forall j = 1, ..., p$, and independently $\theta^{(0)} \sim \mathbf{N}(0, I_p)$.

for t = 0 to N - 1, given $(k^{(t)}, \delta^{(t)}, \theta^{(t)}) = (k, \delta, \theta)$ do

- 1. **Update** δ : Uniformly randomly select a subset J from $\{1, \ldots, p\}$ of size J without replacement, and draw $\bar{\delta} \sim Q_{k,\theta}^{(J)}(\delta, \cdot)$, where the transition kernel described in (17).
- 2. **Update** θ : Draw the components of $[\bar{\theta}]_{\bar{\delta}^c}$ independently from $\mathbf{N}(0, \rho_0^{-1}t_k)$. Draw $[\bar{\theta}]_{\bar{\delta}} \sim P_{\eta_k, k, \bar{\delta}}([\theta]_{\bar{\delta}}, \cdot)$, where $P_{\eta, k, \delta}$ denotes the transition kernel of the MALA with step-size η and invariant distribution given by $W_{k, \delta}$, whose density is proportional to (18).
- 3. Update k: Draw $\bar{k} \sim T_{\bar{\delta},\bar{\theta}}(k,\cdot)$, where $T_{\delta,\theta}$ is the transition kernel of the Metropolis-Hastings on $\{1,\ldots,K\}$ with invariant distribution given by (19) and random walk proposal that has reflection at the boundaries.
- 4. New MCMC state: Set $(\delta^{(t+1)}, \theta^{(t+1)}, k^{(t+1)}) = (\bar{\delta}, \bar{\theta}, \bar{k})$.

end for

Output: $\{(\delta^{(t)}, \theta^{(t)}, k^{(t)}) : 0 \le t \le N \text{ s.t. } k^{(t)} = 1\}$

is the Bernoulli distribution $\mathbf{Ber}(q_i)$, with probability of success given by

$$q_j \stackrel{\text{def}}{=} \left\{ 1 + \exp\left(-\frac{a}{t_k} + \frac{1}{2t_k}(\rho_1 - \rho_0)\theta_j^2\right) \exp\left(\frac{n}{t_k} \mathsf{R}_n(\theta_{\delta^{(j,0)}}; \mathbf{Z}) - \frac{n}{t_k} \mathsf{R}_n(\theta_{\delta^{(j,1)}}; \mathbf{Z})\right) \right\}^{-1}, \quad (15)$$

where

$$\delta_i^{(j,0)} \stackrel{\text{def}}{=} \begin{cases} 0 & i=j \\ \delta_i & i \neq j \end{cases}, \quad \delta_i^{(j,1)} \stackrel{\text{def}}{=} \begin{cases} 1 & i=j \\ \delta_i & i \neq j \end{cases}.$$
 (16)

Given k, θ and j, let $Q_{k,\theta}^{(j)}$ denote the transition kernel on Δ which, given δ , leaves δ_i unchanged for all $i \neq j$, and draws $\delta_j \sim \mathbf{Ber}(q_j)$. We update δ as follows: randomly draw a subset $J = \{J_1, \ldots, J_J\}$ of size J from $\{1, \ldots, p\}$, and update δ using the transition kernel on Δ given by

$$Q_{k,\theta}^{(\mathsf{J})} \stackrel{\text{def}}{=} Q_{k,\theta}^{(\mathsf{J}_1)} Q_{k,\theta}^{(\mathsf{J}_2)} \cdots Q_{k,\theta}^{(\mathsf{J}_J)}. \tag{17}$$

Second, given k and δ , we update θ . We let $[\theta]_{\delta}$ to denote the δ -selected component of θ listed in their original order: $[\theta]_{\delta} \stackrel{\text{def}}{=} (\theta_j : j \in \{1 \le k \le p : \delta_k = 1\})$, and $[\theta]_{\delta^c} \stackrel{\text{def}}{=} (\theta_j : j \in \{1 \le k \le p : \delta_k = 0\})$. We utilize the fact that the selected components $[\theta]_{\delta}$ and the unselected components $[\theta]_{\delta^c}$ of θ are independent conditional on k and δ to update θ . In addition, given k and δ , the components of $[\theta]_{\delta^c}$ are i.i.d. $\mathbf{N}(0, t_k \rho_0^{-1})$ and the distribution of $[\theta]_{\delta}$, denoted by $W_{k,\delta}$, has density on $\mathbb{R}^{\|\delta\|_0}$ proportional to

$$u \mapsto \exp\left(-\frac{\rho_1}{2t_k} \|u\|_2^2 + \frac{n}{t_k} \mathsf{R}_n((u,0)_{\delta}; \mathbf{Z})\right),\tag{18}$$

where the notation $(u,0)_{\delta}$ denotes the vector in \mathbb{R}^p such that $[(u,0)_{\delta}]_{\delta} = u$ and $[(u,0)_{\delta}]_{\delta^c} = \mathbf{0}$. Hence we update $[\theta]_{\delta}$ using a standard Metropolis adjusted Langevin algorithm (MALA) with target distribution $W_{k,\delta}$, and step-size η_k . For details on MALA, see e.g., [31]. For convenience, let us denote the transition kernel of this Markov chain on $\mathbb{R}^{\|\delta\|_0}$ as $P_{\eta_k,k,\delta}$.

Third, given δ and θ , we update k using a standard Metropolis-Hastings algorithm with a random walk proposal that has reflection at the boundaries. Specifically, at k we propose with equal probability either k-1 or k+1, except at 1, where we only propose 2, and at K, where we only propose K-1. Let $T_{\delta,\theta}$ denote the transition kernel on $\{1,\ldots,K\}$ of this Metropolis-Hastings algorithm with invariant distribution

$$i \mapsto \frac{1}{c_i} \exp\left\{\frac{a}{t_i} \|\delta\|_0 - \frac{\rho_1}{2t_i} \|\theta_\delta\|_2^2 - \frac{\rho_0}{2t_i} \|\theta - \theta_\delta\|_2^2 + \frac{n}{t_i} \mathsf{R}_n(\theta_\delta; \mathbf{Z})\right\}.$$
 (19)

Lastly, we collect samples by retaining the values of (δ, θ) at iterations at which k = 1. In stationarity these samples have distribution (8).

3.1 Parameter choices and adaptive tuning

Algorithm 1 as outlined above depends on the user-defined parameters J, K, (t_1, \ldots, t_K) , (c_1, \ldots, c_K) , and (η_1, \ldots, η_K) . The parameter J (the Gibbs sampling batch size) does not greatly impact performance, and setting J = 100 works well in most settings. Efficient selection and tuning of temperatures in simulated tempering has received some attention ([16, 3]), and despite some progress ([24]), to the best of our knowledge, there is no practical and scalable algorithm to do so. In our implementation we use variations of the geometric scaling. We refer the reader to Section 4 for specific choices.

We tune the step-sizes $\eta = (\eta_1, \dots, \eta_K)$ of MALA and the weights (c_1, \dots, c_K) of simulated tempering using adaptive MCMC methods, see e.g., [1]. To tune η_k , we follow the algorithm proposed in [4], with a targeted acceptance probability of 30%. For simulated tempering to visit all temperature levels frequently, the weights (c_1, \dots, c_K) need to be adequately tuned. We refer the reader to [16] for an extensive discussion of the issue. This problem can be efficiently solved using the Wang-Landau algorithm for simulated tempering as developed in [5]. We follow this approach here. The fully adaptive MCMC sampler is presented in Algorithm 2 in the appendix.

3.2 MCMC output processing

Given the output $\{(\delta^{(t)}, \theta^{(t)}, k^{(t)}) : 0 \le t \le N \text{ s.t. } k^{(t)} = 1\}$ from Algorithms 1 or 2, we use three quarters of the total iterations as burn-in. Then we treat the remaining output at iteration $t \in \mathsf{T} \stackrel{\mathrm{def}}{=} \{t : \frac{3}{4}N \le t \le N \text{ s.t. } k^{(t)} = 1\}$ as samples from the distribution of interest in (8). At iteration $t \in \mathsf{T}$, we estimated the principal canonical correlation pair by $v^{(t)}$ where $v^{(t)} \stackrel{\mathrm{def}}{=} [\theta^{(t)}]_{\delta^{(t)}}$ is the entry-wise product of $\delta^{(t)}$ and $\theta^{(t)}$. We denote $v_x^{(t)} \stackrel{\mathrm{def}}{=} (v_i^{(t)} : 1 \le i \le p_x)$ and $v_y^{(t)} \stackrel{\mathrm{def}}{=} (v_i^{(t)} : p_x + 1 \le i \le p)$. Then we normalize $v_x^{(t)}$ and $v_y^{(t)}$ to have unit Euclidean norm as the estimators of $v_{x\star}$ and $v_{y\star}$ at iteration t.

4 Numerical studies

We extensively test the proposed approach. First we test the sample size condition for our algorithm. Since the success of the method is predicated on a good behavior of the MCMC sampler, we investigate empirically the mixing time of Algorithm 1 as the dimension p increases. Then we perform a simulation study that compares our approach to the frequentist method Rifle in [37]. The results clearly show the advantage of using the Raleigh quotient in a Bayesian setting. We also investigate the behavior of the proposed method in settings where one of the datasets is subject to truncation, and we compare the results to the method specifically proposed in [43] to handle such mixed datasets. Again our method outperforms the competition. Our method's implementation is available from the author's github page https://github.com/rachelwho/Sparse-CCA.

4.1 Simulated data generation

We simulate the datasets using a model from [37]. For simplicity, we let $p_x = p_y = p/2$. Then we consider two (p/2)-dimensional random vectors X and Y with joint distribution $(X,Y) \sim \mathbf{N}(0,\Sigma)$. Here we assume that

$$\Sigma = \begin{pmatrix} \Sigma_x & \Sigma_{xy} \\ \Sigma_{xy}^{\mathrm{T}} & \Sigma_y \end{pmatrix}, \quad \Sigma_{xy} = \frac{\lambda_1 \Sigma_x v_{x\star} v_{y\star}^{\mathrm{T}} \Sigma_y}{\sqrt{v_{x\star}^{\mathrm{T}} \Sigma_x v_{x\star}} \sqrt{v_{y\star}^{\mathrm{T}} \Sigma_y v_{y\star}}},$$

where $0 < \lambda_1 < 1$ is the largest generalized eigenvalue, and $v_{x\star}$ and $v_{y\star}$ are the principal canonical correlation vectors. Clearly, $v_{x\star}$ and $v_{y\star}$ are maximizer of the Rayleigh quotient and λ_1 is the maximum value.

We consider the case when Σ_x and Σ_y are block diagonal matrix with five blocks, each of dimension $p/10 \times p/10$, where the (j,j')-th element of each block takes value $0.8^{|j-j'|}$. We let $\lambda_1 = 0.9, (v_{x\star})_j = (v_{y\star})_j = 1/\sqrt{3}$ for $j \in \{1,6,11\}$, and $(v_{x\star})_j = (v_{y\star})_j = 0$ otherwise. Then we generate n samples $(x_i, y_i), i = 1, \ldots, n$ from $\mathbf{N}(0, \Sigma)$.

4.2 Sample size condition

As mentioned above, it was conjectured by ([14]) that it is not possible to construct an estimator of θ_{\star} that is computable in polynomial time and estimates θ_{\star} at the rate ϵ obtained in (13) in the regime $n = o(s^2 \log(p))$. The authors made a compelling argument for this conjecture by showing that any such estimator for the sparse CCA problem can be used to solve the planted clique problem in a regime where it is widely believed to be computationally intractable. Since our estimator achieves the rate ϵ under the weaker condition $n \geq C_0 s \log(p)$, we have the opportunity to test empirically [14]'s conjecture. This boils down to the mixing time of the proposed simulated tempering algorithm.

We generate data from the data model described in Section 4.1 for each $p \in \{500, 2000, 5000\}$, with sample size $n = \lceil s_{\star}^{1.5} \log(p) \rceil$ and $n = \lceil s_{\star}^{2.5} \log(p) \rceil$, where we recall that $s_{\star} = 6$. We use the sample covariance matrices as estimators of Σ_x , Σ_y , and Σ_{xy} to construct the extended posterior distribution $\bar{\Pi}$ in (14) that we sample using Algorithm 2, and temperatures $\{1, 1/0.9, 1/0.8, 1/0.7\}$. Since in this particular data model the largest value of the (population) Rayleigh quotient is $\lambda_1 = 0.9$, we compute the value of the sample Rayleigh quotient $R_n(\cdot; \mathbf{Z})$ along the MCMC iterations and use its proximity to λ_1 as empirical indication of mixing.

We run each MCMC sampler for N = 10,000 iterations, and we repeat each MCMC simulation 30 times (each time with a new dataset). At each iteration time of the MCMC sampler, we average the values of $R_n(\cdot; \mathbf{Z})$ across the 30 replications. Fig. 1 shows the plot of the averaged sample Rayleigh quotient along with iterations. The results seem to suggest that the condition $n \geq C_0 s^2 \log(p)$ is indeed needed for the simulated tempering sampler to mix well, which appears to confirm the conjecture by ([14]).

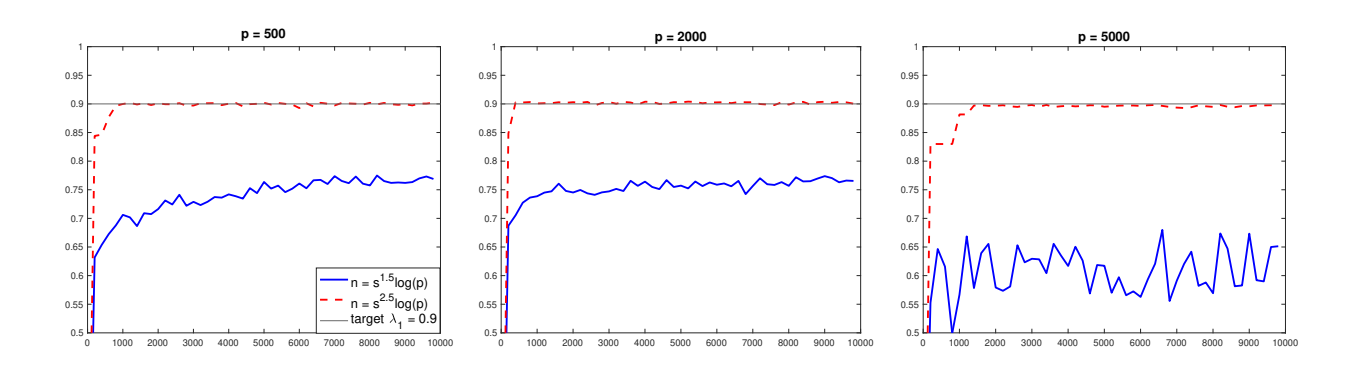


Figure 1: Average values of sample Rayleigh quotient along the MCMC iterations, averaged over 30 data replications.

4.3 Empirical mixing time of Algorithm 1

The simulation results above suggest that the simulated tempering sampler has good mixing properties when the sample size n is large enough. Here we investigate more carefully the mixing time of Algorithm 1 as function of the dimension p, using the coupled chain approach of ([7, 19]). We focus on the case where n = p/2.

We start with a brief description of the method. Let $\{X^{(t)},\ t\geq 0\}$ be the Markov chain generated by Algorithm 1, where $X^{(t)}=(\delta^{(t)},\theta^{(t)},k^{(t)})\in\mathsf{X}$. Let P denote the transition kernel of the Markov chain $\{X^{(t)},\ t\geq 0\}$. The basic idea of the method is to construct a coupling \check{P} of P with itself: that is, a transition kernel on $\mathsf{X}\times\mathsf{X}$ such that $\check{P}((x,y),A\times\mathsf{X})=P(x,A),$ $\check{P}((x,y),\mathsf{X}\times B)=P(y,B),$ for all $x,y\in\mathsf{X},$ and all measurable sets A,B. The coupling \check{P} is constructed in such a way that $\check{P}((x,y),\mathcal{D})>0,$ where $\mathcal{D}\stackrel{\mathrm{def}}{=}\{(x,x):\ x\in\mathsf{X}\}$ and $\check{P}((x,x),\mathcal{D})=1$. The method then proceeds as follows. Fix a lag $L\geq 1.$ Draw $X^{(0)}\sim\bar{\Pi}^{(0)},\ Y^{(0)}\sim\bar{\Pi}^{(0)}$ (where $\bar{\Pi}^{(0)}$ is the initial distribution as given in the initialization step in Algorithm 1). Draw $X^{(k)}|_{(X^{(0)},Y^{(0)})}\sim P^k(X^{(0)},\cdot),$ for all $1\leq k\leq L.$ Then for any $k\geq 1,$ draw,

$$(X_{L+k}, Y_k) | \{(X_{L+k-1}, Y_{k-1}), \dots, (X_L, Y_0)\} \sim \check{P}((X_{L+k-1}, Y_{k-1}), \cdot), \quad k \ge 1.$$

Setting

$$\tau^{(L)} \stackrel{\text{def}}{=} \inf \left\{ k > L : X_k = Y_{k-L} \right\},\,$$

it then holds under some ergodicity assumptions on P (see [7]) that

$$\|\bar{\Pi}^{(t)} - \bar{\Pi}\|_{\mathsf{tv}} \le \mathbb{E}\left[\max\left(0, \left\lceil \frac{\tau^{(L)} - L - t}{L} \right\rceil\right)\right],\tag{20}$$

where $\lceil x \rceil$ denote the smallest integer above x. The implication of (20) is that we can empirically upper bound the left hand side of (20) by simulating multiple copies of the joint chain as described above and then approximating the expectation on the right hand side of (20) by Monte Carlo. We refer the reader to Appendix B for a description of the specific coupled chain that we employ.

Although the empirical mixing time estimation method described above only applies to Markov chains, we have applied it here to the adaptively tuned Algorithm 2. We conjecture that the methodology remains approximately valid for well-constructed adaptive MCMC samplers.

Now we describe the implementation details. We generate datasets from the data model described in Section 4.1 for each $p \in \{100, 200, ..., 5000\}$ with sample size n = p/2. We use sample covariance matrices as estimators of Σ_x , Σ_y , and Σ_{xy} to construct the extended posterior distribution $\bar{\Pi}$ in (14) with temperatures $\{1, 1/0.9, 1/0.8, 1/0.7, 1/0.6\}$. We set the lag L = p and a maximum iterations of $10 \times p + 1000$. For each value of p, we repeat the simulations 50 times to estimate the distribution of the meeting time $\tau^{(L)}$ of the chain. More precisely, using $\varepsilon = 0.1$, we estimate the mixing time of the chain as the first iteration t for which the Monte Carlo estimate of the right hand side of (20) is less than ε . Fig. 2 below shows the plot of the meeting times and the estimated mixing times (both divided by p), as functions of p. The results suggest that Algorithm 2 has a mixing time that scales roughly linearly in the dimension p.

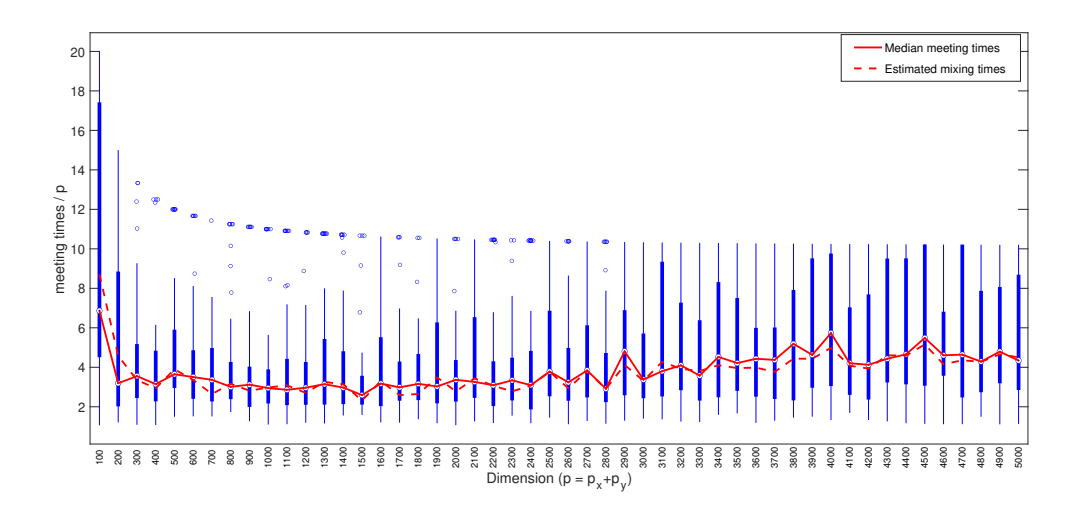


Figure 2: Boxplots of the distributions of meeting times (divided by p) for each value of p. The median meeting time (solid line) as well as the estimated meeting time (dashed line) are also shown.

4.4 Continuous data example and comparison with [37]

We now compare our method to Rifle(k) in [37]. Rifle(k) is a two-stage algorithm. It first solves a convex relaxation of (1). Then using the solution as the initial value, Rifle(k) iteratively perform a gradient ascent step on R_n , and a truncation step that preserves only the top k entries, setting the remaining entries to 0.

We generate the data using the model in Section 4.1, with sample size n = 200 and dimension p = 500. As above we use the sample covariance matrices as estimators of Σ_x , Σ_y , and Σ_{xy} .

Even at this modest scale the computational cost of the first stage of Rifle is high (the running time is about 20 mins using the R-package rifle, compared to about 2 mins for our simulated tempering sampler to converge),

For the MCMC sampling we consider two implementations of Algorithm 2: one without simulated tempering (by only using one temperature, i.e. k=1), and one with simulated tempering by setting the set of temperatures to be $\{1, 1/0.9, 1/0.8, 1/0.7, 1/0.6\}$. We run the MCMC sampler without tempering for number of N=2000 iterations, and N=10000 iterations for simulated tempering. In both case, we process the output as in Section 3.2, then obtaining unit vectors $v_x^{(t)}$ and $v_y^{(t)}$ as estimators of $v_{x\star}$, $v_{y\star}$ at iteration $t \in T$. In the simulated data experiments where the true values of $v_{x\star}$, $v_{y\star}$ are known, we assess the quality of the inference by computing the posterior mean square errors $\widehat{\mathsf{mse}(v_x)}$ and $\widehat{\mathsf{mse}(v_y)}$, where

$$\widehat{\mathsf{mse}(v_x)} \ \stackrel{\mathrm{def}}{=} \ \frac{1}{|\mathsf{T}|} \sum_{t \in \mathsf{T}} \mathsf{mse}(v_x^{(t)}), \quad \text{and} \qquad \mathsf{mse}(v_x) \ \stackrel{\mathrm{def}}{=} \ \min\left(\|v_x - v_{x\star}\|_2^2, \ \|v_x + v_{x\star}\|_2^2\right), \quad (21)$$

and $\widehat{\mathsf{mse}(v_y)}$ is computed similarly.

For the comparison we use Rifle(6) (that is the method is provided with the exact number of nonzero components). Because of the high computational cost of Rifle we explored two possibilities. In the first experiment, the initial estimate in Rifle(6) is generated from mean zero standard Gaussian noise, the same as our simulated tempering sampler. In the second experiment, we initialize Rifle(6) from the ground truth $v_{x\star}$, $v_{y\star}$ perturbed with mean zero Gaussian noise with standard deviation 0.2. In such initialization, the elements of the initial value at indices i where $\theta_{\star i} \neq 0$ will be greater than $1/\sqrt{3} - 0.2 * 1.5 \approx 0.3$ with probability over 93%, and the elements of the initial value at indices i where $\theta_{\star i} = 0$ will be less than 0.2 * 1.5 = 0.3 with probability over 93%. Hence after truncation, the support of the initial value is the true support of θ_{\star} with high probability, which assures the goodness of the initial estimate in the second experiment. As with our method we report the mean square errors of Rifle (see Equation (21)). These mean square errors estimates are then averaged over 100 data simulations. The results are shown in Table 1.

We can see from the results that Rifle(6) typically requires a good initialization and performs very poorly otherwise. However, even with good initialization the method still significantly underperforms our Bayesian method. The results also illustrate the advantage of using simulated tempering. In roughly one out of four datasets the plain MCMC sampler – without tempering – gets trapped in a local mode. This explains its relatively poor performance.

	Rifle(6) with random Init.	Rifle(6) with good Init.	MCMC	Simulated Temp.
$mse(v_x)$	1.38 (0.31)	0.32 (0.25)	0.50 (0.80)	0.06 (0.28)
$mse(v_y)$	1.40 (0.31)	$0.31\ (0.27)$	0.48 (0.81)	$0.06 \ (0.28)$

Table 1: Mean square errors of Rifle(6) and proposed Bayesian method. The algorithm Rifle(6) is initialized either from random noise (first column), or from the truth plus a small noise (2nd column). The numbers in parenthesis are standard errors obtained from 100 data replications.

4.5 Application to mixed data type and comparison with [43]

In this section, we investigate the performance of our method when the data generating process deviates from the multivariate Gaussian generator described in Section 4.1. We consider the truncated latent Gaussian copula model in [43]. The truncated latent Gaussian copula model is useful in modeling truncated and non-Gaussian data, which are commonly encountered in biomedical applications. Our proposed framework remains easily applicable to this model.

Definition 6 (Gaussian copula model). A random vector $Z = (Z_1, \ldots, Z_p)^{\mathrm{T}}$ is a realization of the Gaussian copula model, if there exists a transformation $h : \mathbb{R}^p \to \mathbb{R}^p$ such that $h(Z) = (h_1(Z_1), \ldots, h_p(Z_p))^{\mathrm{T}} \sim \mathbf{N}(0, \Sigma)$ and for each $j = 1, \ldots, p$, transformation $h_j : \mathbb{R} \to \mathbb{R}$ is monotonically increasing. We write this as $Z \sim \mathbf{NPN}(0, \Sigma, h)$.

Definition 7 (Truncated Gaussian copula model). A random vector $Z = ((Z^{(1)})^T, (Z^{(2)})^T)^T$, where $Z^{(1)} \in \mathbb{R}^{p_x}$ and $Z^{(2)} \in \mathbb{R}^{p_y}$, is a realization of a latent Gaussian copula model with truncation if there exists a random vector $U \in \mathbb{R}^{p_y}$ such that $(Z^{(1)}, U) \sim \mathbf{NPN}(0, \Sigma, h)$ and $Z_j^{(2)} = I(U_j > C_j)U_j$ for all $j = 1, \ldots, p_y$, where $C = (C_1, \ldots, C_{p_y})$ is a truncation parameter. We write $Z \sim \mathbf{TNPN}(0, \Sigma, h, C)$.

In this model the parameter of interest is the principal canonical correlation vectors of $h(Z^{(1)}, U) \sim \mathbf{N}(0, \Sigma)$. However the challenge is that we can only observe Z. Building on the work by ([22, 11]) it is shown by [43] that a Kendall's-tau-based estimator of the covariance matrix Σ can be derived from n realizations of $Z \sim \mathbf{TNPN}(0, \Sigma, h, C)$. We refer the reader to [43] for details. Let $\hat{\Sigma} = \begin{pmatrix} \hat{\Sigma}_x & \hat{\Sigma}_{xy} \\ \hat{\Sigma}_{yx} & \hat{\Sigma}_y \end{pmatrix}$ be the resulting estimator, where $\hat{\Sigma}_x$ and $\hat{\Sigma}_{xy}$ are estimators for covariance matrix of X and Y and $\hat{\Sigma}_y$ is the estimator between X and Y. Based on $\hat{\Sigma}_x, \hat{\Sigma}_{xy}$ and $\hat{\Sigma}_y$, our methodology readily applies, leading to the quasi-posterior distribution (8) and a similar estimator $\hat{\mathcal{P}}$. We compare our approach to the estimator proposed by [43] that estimates the principal canonical correlation pair by solving

$$\max_{v_x, v_y} v_x^{\mathrm{T}} \hat{\Sigma}_{xy} v_y - \lambda_1 \|v_x\|_1 - \lambda_2 \|v_y\|_1, \quad \text{s.t.} \quad v_x^{\mathrm{T}} \hat{\Sigma}_x v_x \le 1, \quad v_y^{\mathrm{T}} \hat{\Sigma}_y v_y \le 1.$$
 (22)

For the comparison we set sample size n=200 and dimensions $p_x, p_y=100$, and generate the dataset from $\mathbf{TNPN}(0, \Sigma, h, C)$, where Σ is constructed the same way in Section 4.1. As shown in [43], since the Kendall's-tau-based estimator $\hat{\Sigma}$ is invariant to h, without any loss of generality, we set h to be identity function. For simplicity, we only test for $C=c\mathbf{1}_{p_y}$, where c=-2,-1,0. The resulting truncation level (percentage of zero elements across the variables) is in the range of 2-50%.

Truncation		Simulated tempering		mixedcc	a(BIC1)	mixedcca(BIC2)	
c	truncation level	$\widehat{mse(v_x)}$	$\widehat{mse(v_y)}$	$mse(v_y)$	$mse(v_x)$	$mse(v_y)$	$mse(v_x)$
-2	0.02	0.02 (0.00)	0.02 (0.01)	0.04 (0.03)	0.04 (0.05)	0.04 (0.03)	0.04 (0.04)
-1	0.16	0.02 (0.01)	0.03 (0.01)	0.04 (0.03)	0.04 (0.04)	0.04 (0.03)	0.05 (0.04)
0	0.50	0.03 (0.01)	0.11 (0.03)	0.07 (0.05)	0.11 (0.13)	0.08 (0.05)	$0.12 \; (\; 0.12 \;)$

(a) mse

	Truncation	Simulated tempering		mixedcca(BIC1)		mixedcca(BIC2)	
c	truncation level	$\widehat{TPR(v_x)}$	$\widehat{TPR(v_y)}$	$TPR(v_x)$	$TPR(v_y)$	$TPR(v_x)$	$TPR(v_y)$
-2	0.02	1.00 (0.00)	1.00 (0.01)	1.00 (0.00)	1.00 (0.00)	1.00 (0.00)	1.00 (0.00)
-1	0.16	1.00 (0.00)	1.00 (0.02)	1.00 (0.00)	1.00 (0.00)	1.00 (0.00)	1.00 (0.00)
0	0.50	1.00 (0.01)	0.96 (0.10)	1.00 (0.00)	1.00 (0.00)	1.00 (0.00)	1.00 (0.00)

(b) TPR

	Truncation	Simulated tempering		mixedcca(BIC1)		mixedcca(BIC2)	
c	truncation level	$\widehat{TNR(v_x)}$	$\widehat{TNR(v_y)}$	$TNR(v_x)$	$TNR(v_y)$	$TNR(v_x)$	$TNR(v_y)$
-2	0.02	1.00 (0.00)	1.00 (0.00)	0.98 (0.01)	0.98 (0.01)	0.97 (0.02)	0.96 (0.02)
-1	0.16	1.00 (0.00)	1.00 (0.00)	0.98 (0.01)	0.98 (0.01)	0.96 (0.02)	0.96 (0.02)
0	0.50	1.00 (0.00)	1.00 (0.00)	0.98 (0.01)	0.97 (0.02)	0.94 (0.03)	0.93 (0.05)

(c) TNR

Table 2: Mean (and standard deviation) of $\widehat{\mathsf{mse}}$, $\widehat{\mathsf{TPR}}$ and $\widehat{\mathsf{TNR}}$ of proposed method and mse , TPR and TNR of $\widehat{\mathsf{mixedCCA}}$ for different truncation values c when h is identity function.

We implement Algorithm 2 with the number of iterations N=10000 and the set of temperatures $\{1,1/0.9,1/0.8,1/0.7\}$. We evaluate the quality of the inference by computing the posterior mean square errors $\widehat{\mathsf{mse}(v_x)}$ and $\widehat{\mathsf{mse}(v_y)}$ as in (21). We also assess the variable selection performance at iteration $t\in\mathsf{T}$ by computing true-positive rate (TPR) and true-negative rate (TNR) defined as

$$\mathsf{TPR}(v_x^{(t)}) \stackrel{\text{def}}{=} \frac{\#\{j: (v_x^{(t)})_j \neq 0, (v_{x\star})_j \neq 0\}}{\#\{j: (v_{x\star})_j \neq 0\}}, \ \ \mathsf{TNR}(v_x^{(t)}) \stackrel{\text{def}}{=} \frac{\#\{j: (v_x^{(t)})_j = 0, (v_{x\star})_j = 0\}}{\#\{j: (v_{x\star})_j = 0\}}, \ \ (23)$$

and $\mathsf{TPR}(v_y^{(t)})$, $\mathsf{TNR}(v_y^{(t)})$ is computed similarly. We assess the algorithm performance by averaging TPR and TNR over $t \in \mathsf{T}$, denoted $\widehat{\mathsf{TPR}}$ and $\widehat{\mathsf{TNR}}$.

For the comparison we compute the estimator (22) using the algorithm mixedcca in the R package mixedCCA of [43], using BIC1 and BIC2 criteria respectively for selecting the regularization parameters λ_1 and λ_2 . We average these performance measures over 50 data replications, and the results are presented in Table 2. We can see from Table 2a that overall our approach performs better than mixedcca in terms of accuracy, in particular with smaller standard deviation.

5 Principal canonical correlation of clinical and proteomic data in covid-19 patients

COVID-19 is an infectious disease that is rapidly sweeping through the world. The disease is caused by a severe acute respiratory syndrome coronavirus (SARS-CoV-2). There is currently an intense global effort to better understand the virus and find cures and vaccines. We use our methodology to re-analysis a data set produced by [36] that aims to identify biomarkers for early detection of severely ill Covid-19 patients¹. To that end, the study enrolled 86 patients (some non-Covid-19 patients, and among the Covid-19 patients, some that developed mild symptoms, and some that became severely ill). The exact protocol for recruiting these patients is unclear. For each patient they measured three (3) physical characteristics (sex, age, and body mass index), twelve (12) clinical variables as routinely measured from blood samples (white blood cells count, lymphocytes count, C-reactive protein, etc...). Furthermore, the serum of each patient is analyzed by liquid mass spectrometry-based proteomics to quantify their proteome and metabolome. In [36], the data is used to build a statistical model to predict whether or not a Covid-19 patient will progress to a severe state of illness. The dataset of [36] is freely available from the journal website.

We use canonical correlation analysis to re-analyze the data. A common working assumption is that SARS-CoV-2 induces patterns of molecular changes that can be detected in the sera of patients. Canonical correlation analysis may help identify these patterns. To do this we focus on the proteomic data, and we estimate the principal sparse canonical correlation between the physical and clinical variables on one hand and the proteomic variables on the other. See for instance [32] for a similar analysis on tuberculosis and malaria.

We pre-process the data by removing all the proteins for which 50% or more values are missing, leading to a total of $p_y = 513$ proteins, and $p_x = 15$ clinical and physical variables. The sample size is n = 86 patients. Liquid mass spectrometry-based proteomics typically produces a large quantity of missing values ([20, 27]). We make the assumption here that the missing values are driven mainly by detection limit truncation ([20]), which makes the truncated latent Gaussian copula model described above appropriate for this example. We apply simulated tempering with temperatures $\{1, 1/0.9, 1/0.8, 1/0.7\}$ that we run for 100,000 iterations.

Our estimate of the principal canonical vector of first dataset $(v_{x\star})$ has only one selected component (corresponding to C-reactive protein) with estimated inclusion probability of $\Pi(\delta_j = 1|\mathbf{Z}) = 0.99$. All other physical and clinical variables have inclusion probabilities smaller than 0.1. We found also that the principal canonical vector of the proteomic data is also driven by a single protein (P02763, also known as Alpha-1-acid glycoprotein 1 or AGP 1), with estimated inclusion probability of $\Pi(\delta_j = 1|\mathbf{Z}) = 0.89$. All other proteins have inclusion probability smaller than 0.1. Fig. 3 shows the boxplot of the distribution of sample Rayleigh quotient (this corresponds to the estimated correlation $\hat{\rho}$ between the two data set), as well as the boxplot and autocorrelation function of the MCMC output of the coefficients of CRP and AGP 1 in the quasi-posterior distribution. The fast decay of the autocorrelation functions show a good mixing of the MCMC sampler.

¹For reasons that are still poorly understood, about 80% of patients infected by SARS-CoV-2 experience mild to no symptoms, whereas in about 20% of the cases, patients become severely ill.

The highly sparse nature of the estimated canonical correlation vectors is striking. Several studies have observed the predictive power of C-reative protein (CRP) in the progression of Covid-19 into a severe illness (see for instance [34] for a meta-analysis). This suggests that the correlation detected in our analysis between the two datasets is indeed driven by the progression of Covid-19 into a severe illness. Therefore, our analysis suggests that protein AGP 1 may also be playing an important role in the progression of Covid-19 into a severe illness. We learn from Uniprot², that AGP 1 functions as transport protein in the blood stream, and appears to function in modulating the activity of the immune system during the acute-phase reaction. Furthermore, AGP 1 appears on the list of differentially expressed proteins in the sera of severely ill Covid-19 patients designed by [36], and also appeared in the literature as playing a role in the immune system's response to malaria ([12]).

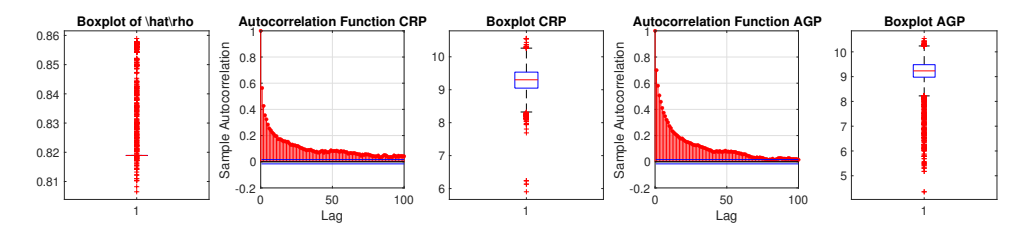


Figure 3: Boxplot and autocorrelation plots from MCMC output.

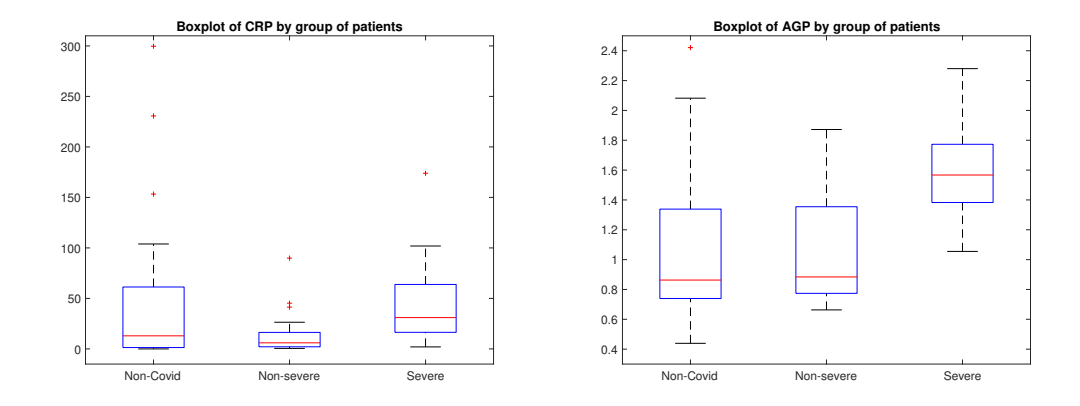


Figure 4: Distribution of CRP and AGP by group of patients.

6 Conclusion

In this work, we have developed a minimax optimal estimation procedure for sparse canonical correlation analysis within a quasi-Bayesian framework. Our method can be further extended to capture more than one canonical correlation vector, either by deflation, or by reformulating

²https://www.uniprot.org

the problem as a higher dimensional canonical correlation analysis estimation problem as in [37]. Also, one can straightforwardly extend our method to solve other generalized eigenvalue problems that arise in other statistical problems, as for instance in Fisher discriminant analysis. Finally whether it is possible to use the full quasi-posterior distribution for a Bayesian inference of θ_{\star} in the high-dimensional setting is an important problem that we leave for possible future research.

7 Acknowledgements

The authors are grateful to Roger Zoh for very helpful discussions. This work is partially supported by the NSF grant DMS 2015485.

References

- [1] Christophe Andrieu and Johannes Thoms. A tutorial on adaptive mcmc. Statistics and Computing, 18(4):343–373, 2008.
- [2] Yves Atchadé and Anwesha Bhattacharyya. An approach to large-scale quasi-bayesian inference with spike-and-slab priors, 2019.
- [3] Yves Atchadé, Gareth Roberts, and Jeffrey Rosenthal. Towards optimal scaling of metropolis-coupled markov chain monte carlo. *Statistics and Computing*, 21:555–568, 10 2011.
- [4] Yves Atchadé and Jeffrey Rosenthal. On adaptive markov chain monte carlo algorithms. Bernoulli, 11, 10 2005.
- [5] Yves F. Atchadé and Jun S. Liu. The wang-landau algorithm in general state spaces: Applications and convergence analysis. *Statistica Sinica*, 20(1):209–233, 2010.
- [6] P. G. Bissiri, C. C. Holmes, and S. G. Walker. A general framework for updating belief distributions. Journal of the Royal Statistical Society: Series B (Statistical Methodology), 78(5):1103–1130, 2016.
- [7] Niloy Biswas, Pierre E. Jacob, and Paul Vanetti. Estimating convergence of markov chains with l-lag couplings, 2019.
- [8] B. P. Carlin and S. Chib. Bayesian model choice via markov chain monte carlo methods. *J. Roy. Stat. Soc. B*, 57(3):473–484, 1995.
- [9] Olivier Catoni. Statistical learning theory and stochastic optimization, volume 1851 of Lecture Notes in Mathematics. Springer-Verlag, Berlin, 2004. Lecture notes from the 31st Summer School on Probability Theory held in Saint-Flour, July 8–25, 2001.

- [10] Victor Chernozhukov and Han Hong. An MCMC approach to classical estimation. *J. Econometrics*, 115(2):293–346, 2003.
- [11] Jianqing Fan, Han Liu, Yang Ning, and Hui Zou. High dimensional semiparametric latent graphical model for mixed data. *Journal of the Royal Statistical Society: Series B (Statistical Methodology)*, 79(2):405–421, 2017.
- [12] M J Friedman. Control of malaria virulence by alpha 1-acid glycoprotein (orosomucoid), an acute-phase (inflammatory) reactant. Proceedings of the National Academy of Sciences, 80(17):5421-5424, 1983.
- [13] Chao Gao, Zongming Ma, Zhao Ren, and Harrison H. Zhou. Minimax estimation in sparse canonical correlation analysis. *Ann. Statist.*, 43(5):2168–2197, 10 2015.
- [14] Chao Gao, Zongming Ma, and Harrison H. Zhou. Sparse cca: Adaptive estimation and computational barriers. *Ann. Statist.*, 45(5):2074–2101, 10 2017.
- [15] Edward I. George and Robert E. McCulloch. Approaches for bayesian variable selection. Statistica Sinica, 7(2):339–373, 1997.
- [16] Charles J. Geyer and Elizabeth A. Thompson. Annealing markov chain monte carlo with applications to ancestral inference. *Journal of the American Statistical Association*, 90(431):909–920, 1995.
- [17] David Hardoon and John Shawe-Taylor. Sparse canonical correlation analysis. *Machine Learning*, 83:331–353, 06 2011.
- [18] H Hotelling. Relations between two sets of variates. Biometrika, 1936.
- [19] Pierre Jacob, John O'Leary, and Yves Atchadé. Unbiased markov chain monte carlo with couplings. Journal of the Royal Statistical Society: Series B (Statistical Methodology), 08 2017.
- [20] Yuliya V. Karpievitch, Ashoka D. Polpitiya, Gordon A. Anderson, Richard D. Smith, and Alan R. Dabney. Liquid chromatography mass spectrometry-based proteomics: Biological and technological aspects. *Ann. Appl. Stat.*, 4(4):1797–1823, 12 2010.
- [21] Shengqiao Li. Concise formulas for the area and volume of a hyperspherical cap. *Asian Journal of Mathematics and Statistics*, 4(1):66–70, 2011.
- [22] Han Liu, John Lafferty, and Larry Wasserman. The nonparanormal: Semiparametric estimation of high dimensional undirected graphs. *Journal of Machine Learning Research*, 10, 04 2009.
- [23] David A. McAllester. Some pac-bayesian theorems. Machine Learning, 37(3):355–363, 1999.
- [24] Btażej Miasojedow, Eric Moulines, and Matti Vihola. An adaptive parallel tempering algorithm. *Journal of Computational and Graphical Statistics*, 22(3):649–664, 2013.

- [25] T. J. Mitchell and J. J. Beauchamp. Bayesian variable selection in linear regression. JASA, 83(404):1023–1032, 1988.
- [26] Qianxing Mo, Ronglai Shen, Cui Guo, Marina Vannucci, Keith S Chan, and Susan G Hilsenbeck. A fully bayesian latent variable model for integrative clustering analysis of multi-type omics data. *Biostatistics*, 19(1):71–86, 2017.
- [27] Jonathon J. O'Brien, Harsha P. Gunawardena, Joao A. Paulo, Xian Chen, Joseph G. Ibrahim, Steven P. Gygi, and Bahjat F. Qaqish. The effects of nonignorable missing data on label-free mass spectrometry proteomics experiments. *Ann. Appl. Stat.*, 12(4):2075–2095, 12 2018.
- [28] Elena Parkhomenko, David Tritchler, and Joseph Beyene. Sparse canonical correlation analysis with application to genomic data integration. *Statistical applications in genetics and molecular biology*, 8:Article 1, 2009.
- [29] Nimrod Rappoport and Ron Shamir. Multi-omic and multi-view clustering algorithms: review and cancer benchmark. *Nucleic acids research*, 46(20):10546–10562, 2018.
- [30] Garvesh Raskutti, Martin J. Wainwright, and Bin Yu. Restricted eigenvalue properties for correlated gaussian designs. *J. Mach. Learn. Res.*, 11:2241–2259, 2010.
- [31] Gareth O. Roberts and Richard L. Tweedie. Exponential convergence of langevin distributions and their discrete approximations. *Bernoulli*, 2(4):341–363, 1996.
- [32] Juho Rousu, Daniel D. Agranoff, Olugbemiro Sodeinde, John Shawe-Taylor, and Delmiro Fernandez-Reyes. Biomarker discovery by sparse canonical correlation analysis of complex clinical phenotypes of tuberculosis and malaria. *PLOS Computational Biology*, 9(4):1–10, 04 2013.
- [33] Mark Rudelson and Shuheng Zhou. Reconstruction from anisotropic random measurements. *IEEE Trans. Inf. Theor.*, 59(6):3434–3447, June 2013.
- [34] Bikash R. Sahu, Raj Kishor Kampa, Archana Padhi, and Aditya K. Panda. C-reactive protein: A promising biomarker for poor prognosis in covid-19 infection. *Clinica Chimica Acta*, 509:91 – 94, 2020.
- [35] Benjamin A. Shaby. The open-faced sandwich adjustment for mcmc using estimating functions. *Journal of Computational and Graphical Statistics*, 23(3):853–876, 10 2014.
- [36] Bo Shen, Xiao Yi, Yaoting Sun, Xiaojie Bi, Juping Du, Chao Zhang, Sheng Quan, Fangfei Zhang, Rui Sun, Liujia Qian, Weigang Ge, Wei Liu, Shuang Liang, Hao Chen, Ying Zhang, Jun Li, Jiaqin Xu, Zebao He, Baofu Chen, Jing Wang, Haixi Yan, Yufen Zheng, Donglian Wang, Jiansheng Zhu, Ziqing Kong, Zhouyang Kang, Xiao Liang, Xuan Ding, Guan Ruan, Nan Xiang, Xue Cai, Huanhuan Gao, Lu Li, Sainan Li, Qi Xiao, Tian Lu, Yi Zhu, Huafen Liu, Haixiao Chen, and Tiannan Guo. Proteomic and metabolomic characterization of covid-19 patient sera. *Cell*, 182(1):59 72.e15, 2020.

- [37] Kean Ming Tan, Zhaoran Wang, Han Liu, and Tong Zhang. Sparse generalized eigenvalue problem: Optimal statistical rates via truncated rayleigh flow. *Journal of the Royal Statistical Society: Series B (Statistical Methodology)*, 80(5):1057–1086, 2018.
- [38] Roman Vershynin. High-Dimensional Probability: An Introduction with Applications in Data Science. Cambridge Series in Statistical and Probabilistic Mathematics. Cambridge University Press, 2018.
- [39] Vincent Q. Vu and Jing Lei. Minimax sparse principal subspace estimation in high dimensions. *Ann. Statist.*, 41(6):2905–2947, 12 2013.
- [40] Sandra Waaijenborg and Aeilko Zwinderman. Sparse canonical correlation analysis for identifying, connecting and completing gene-expression networks. BMC bioinformatics, 10:315, 09 2009.
- [41] Ami Wiesel, Mark Kliger, and Alfred Hero. A greedy approach to sparse canonical correlation analysis. 02 2008.
- [42] Daniela M Witten and Robert J Tibshirani. Extensions of sparse canonical correlation analysis with applications to genomic data. Statistical applications in genetics and molecular biology, 8(1):1–27, 2009.
- [43] Grace Yoon, Raymond J. Carroll, and Irina Gaynanova. Sparse semiparametric canonical correlation analysis for data of mixed types. arXiv: Methodology, 2018.

A Proof of Theorem 4

Throughout the proof c_0 denotes a generic absolute constant that depends only on $\underline{\kappa}$ and $\bar{\kappa}$ in H2, but whose actual value or expression may change during the text.

For $\delta \in \Delta_s$, let

$$\mathsf{B}_{\delta} \stackrel{\mathrm{def}}{=} \left\{ \theta \in \mathbb{R}^p: \ M\epsilon < \left\| \frac{\theta_{\delta}\theta_{\delta}^{\mathrm{T}}}{\|\theta_{\delta}\|_2^2} - \theta_{\star}\theta_{\star}^{\mathrm{T}} \right\|_{\mathsf{F}} \right\},$$

and

$$\mathsf{B} \stackrel{\mathrm{def}}{=} \cup_{\delta \in \Delta_s} \{\delta\} \times \mathsf{B}_{\delta}.$$

By splitting the integral over B, B^c and the remaining space we obtain

$$\int_{\Delta_{s} \times \mathbb{R}^{p}} \left\| \frac{\theta_{\delta} \theta_{\delta}^{\mathrm{T}}}{\theta_{\delta}^{\mathrm{T}} \theta_{\delta}} - \theta_{\star} \theta_{\star} \right\|_{\mathsf{F}} \Pi\left(\mathrm{d}\delta, \mathrm{d}\theta | \mathbf{Z}\right) \leq M\epsilon + \Pi(\mathsf{B}|\mathbf{Z}). \tag{24}$$

We then proceed to bound $\Pi(B|\mathbf{Z})$. From the definition of $\Pi(\cdot|\mathbf{Z})$ and by integrating out the non-selected component $\theta - \theta_{\delta}$, we have

$$\Pi(\mathsf{B}|\mathbf{Z}) = \frac{\sum_{\delta \in \Delta_s} e^{\mathsf{a}\|\delta\|_0} \int_{\mathbb{R}^p} \mathbf{1}_{\mathsf{B}_{\delta}}(\theta) \exp\left(-\frac{\rho_1}{2} \|\theta_{\delta}\|_2^2 - \frac{\rho_0}{2} \|\theta - \theta_{\delta}\|_2^2 + n\mathsf{R}_n(\theta_{\delta}; \mathbf{Z})\right) d\theta}{\sum_{\delta \in \Delta_s} e^{\mathsf{a}\|\delta\|_0} \int_{\mathbb{R}^p} \exp\left(-\frac{\rho_1}{2} \|\theta_{\delta}\|_2^2 - \frac{\rho_0}{2} \|\theta - \theta_{\delta}\|_2^2 + n\mathsf{R}_n(\theta_{\delta}; \mathbf{Z})\right) d\theta} \\
= \frac{\sum_{\delta \in \Delta_s} \left(\frac{1}{p^{\mathsf{u}}} \sqrt{\frac{\rho_1}{2\pi}}\right)^{\|\delta\|_0} \int_{\mathbb{R}^{\|\delta\|_0}} \mathbf{1}_{\mathsf{B}_{\delta}}((u, 0)_{\delta}) \exp\left(-\frac{\rho_1}{2} \|u\|_2^2 + n\bar{\mathsf{R}}_n((u, 0)_{\delta}; \mathbf{Z})\right) du}{\sum_{\delta \in \Delta_s} \left(\frac{1}{p^{\mathsf{u}}} \sqrt{\frac{\rho_1}{2\pi}}\right)^{\|\delta\|_0} \int_{\mathbb{R}^{\|\delta\|_0}} \exp\left(-\frac{\rho_1}{2} \|u\|_2^2 + n\bar{\mathsf{R}}_n((u, 0)_{\delta}; \mathbf{Z})\right) du}, \quad (25)$$

where

$$\bar{\mathsf{R}}_n(\theta; \mathbf{Z}) \stackrel{\mathrm{def}}{=} \mathsf{R}_n(\theta; \mathbf{Z}) - \mathsf{R}_n(\theta_\star; \mathbf{Z}).$$

We show in Lemma 8 that the denominator on the right hand side of (25) is bound from below by $e^{-(s_{\star}+1)(\mathsf{u}+1)\log(p\vee(c_0n))}$, for some absolute constant c_0 . This implies that

 $\Pi(\mathsf{B}|\mathbf{Z}) \le e^{(s_{\star}+1)(\mathsf{u}+1)\log(p\vee(c_0n))}$

$$\times \sum_{\delta \in \Delta_{\delta}} \left(\frac{1}{p^{\mathsf{u}}} \sqrt{\frac{\rho_{1}}{2\pi}} \right)^{\|\delta\|_{0}} \int_{\mathbb{R}^{\|\delta\|_{0}}} \mathbf{1}_{\mathsf{B}_{\delta}}((u,0)_{\delta}) \exp\left(-\frac{\rho_{1}}{2} \|u\|_{2}^{2} + n\bar{\mathsf{R}}_{n}((u,0)_{\delta}; \mathbf{Z}) \right) du. \tag{26}$$

We show in Lemma 11 that any $\theta \in \mathbb{R}^p$, such that $\|\theta\|_0 \leq s$,

$$\mathsf{R}_n(\theta;\mathbf{Z}) - \mathsf{R}_n(\theta_\star;\mathbf{Z}) \leq -\frac{\mathsf{gap}}{2} \left(\frac{\underline{\kappa}}{\bar{\kappa}}\right)^2 \|\theta\theta^{\scriptscriptstyle \mathrm{T}} - \theta_\star \theta_\star^{\scriptscriptstyle \mathrm{T}}\|_{\mathsf{F}}^2 + c_0 \mathsf{r}_1 \|\theta\theta^{\scriptscriptstyle \mathrm{T}} - \theta_\star \theta_\star^{\scriptscriptstyle \mathrm{T}}\|_{\mathsf{F}},$$

for some absolute constant c_0 that depends only on $\underline{\kappa}$ and $\bar{\kappa}$. Therefore, for $\frac{4c_0\mathsf{r}_1}{\mathsf{gap}}\left(\frac{\bar{\kappa}}{\underline{\kappa}}\right)^2 \leq \|\theta\theta^{\mathrm{T}} - \theta_{\star}\theta_{\star}^{\mathrm{T}}\|_{\mathsf{F}}$, we have

$$\mathsf{R}_n(\theta; \mathbf{Z}) - \mathsf{R}_n(\theta_\star; \mathbf{Z}) \leq -\frac{\mathsf{gap}}{4} \left(\frac{\underline{\kappa}}{\bar{\kappa}}\right)^2 \|\theta\theta^{\mathrm{\scriptscriptstyle T}} - \theta_\star \theta_\star^{\mathrm{\scriptscriptstyle T}}\|_{\mathsf{F}}^2.$$

Therefore, for $M \geq 4c_0 \left(\frac{\bar{\kappa}}{\kappa}\right)^2$, we have

$$\begin{split} \Pi(\mathsf{B}|\mathbf{Z}) & \leq e^{(s_\star + 1)(\mathsf{u} + 1)\log(p\vee(c_0n))} \\ & \times e^{-\frac{M^2\mathsf{gap}}{4}\left(\frac{\kappa}{\overline{\kappa}}\right)^2n\epsilon^2} \sum_{\delta \in \Delta_s} \left(\frac{1}{p^\mathsf{u}}\sqrt{\frac{\rho_1}{2\pi}}\right)^{\|\delta\|_0} \int_{\mathbb{R}^{\|\delta\|_0}} \mathbf{1}_{\mathsf{B}_\delta}((u,0)_\delta) \exp\left(-\frac{\rho_1}{2}\|u\|_2^2\right) \mathrm{d}u \\ & \leq e^{(s_\star + 1)(\mathsf{u} + 1)\log(p\vee(c_0n))} e^{-\frac{M^2\mathsf{gap}}{4}\left(\frac{\kappa}{\overline{\kappa}}\right)^2n\epsilon^2} \sum_{\delta \in \Delta_s} \left(\frac{1}{p^\mathsf{u}}\sqrt{\frac{\rho_1}{2\pi}}\right)^{\|\delta\|_0} \left(2\pi\rho_1^{-1}\right)^{\|\delta\|_0/2} \\ & < 2e^{(s_\star + 1)(\mathsf{u} + 1)\log(p\vee(c_0n))} e^{-\frac{M^2\mathsf{gap}}{4}\left(\frac{\kappa}{\overline{\kappa}}\right)^2n\epsilon^2} < 2e^{-\frac{M^2}{8\mathsf{gap}}\left(\frac{\kappa}{\overline{\kappa}}\right)^2nr_1^2}, \end{split}$$

under the sample size condition (12), where the third inequality follows from the assumptions u > 1, and $p^{u-1} > 2$.

The theorem follows by collecting the terms.

We derive here a lower bound on the normalizing constant of the quasi-posterior distribution.

Lemma 8. Under Assumption H2, and assuming that $p^{\mathsf{u}} \geq e^1 s_{\star}$, we have

$$\sum_{\delta \in \Delta_{s}} \left(\frac{1}{p^{\mathsf{u}}} \sqrt{\frac{\rho_{1}}{2\pi}} \right)^{\|\delta\|_{0}} \int_{\mathbb{R}^{\|\delta\|_{0}}} \exp\left(-\frac{\rho_{1}}{2} \|u\|_{2}^{2} + n\bar{R}_{n}((u,0)_{\delta};\mathbf{Z}) \right) du \ge e^{-(s_{\star}+1)(\mathsf{u}+1)\log(p\vee(c_{0}n))}, \quad (27)$$

for some absolute constant c_0 .

Proof. Clearly, the left hand side of (27) is bounded from below by

$$\left(\frac{1}{p^{\mathsf{u}}}\sqrt{\frac{\rho_1}{2\pi}}\right)^{s_{\star}} \int_{\mathbb{R}^{s_{\star}}} \exp\left(-\frac{\rho_1}{2}||u||_2^2 + n\bar{\mathsf{R}}_n((u,0)_{\delta_{\star}};\mathbf{Z})\right) du.$$

For any $\theta \in \mathbb{R}^p$ that has the same support as θ_{\star} , we have

$$\begin{split} \bar{\mathsf{R}}_{n}(\theta;\mathbf{Z}) &= \frac{\theta^{\mathsf{T}}\hat{A}\theta}{\theta^{\mathsf{T}}\hat{B}\theta} - \frac{\theta_{\star}^{\mathsf{T}}\hat{A}\theta_{\star}}{\theta_{\star}^{\mathsf{T}}\hat{B}\theta_{\star}} \\ &= \frac{\theta^{\mathsf{T}}\hat{\Sigma}\theta}{\theta^{\mathsf{T}}\hat{B}\theta} - \frac{\theta_{\star}^{\mathsf{T}}\hat{\Sigma}\theta_{\star}}{\theta_{\star}^{\mathsf{T}}\hat{B}\theta_{\star}} \\ &= \frac{\theta^{\mathsf{T}}\hat{\Sigma}\theta\left(\theta_{\star}^{\mathsf{T}}\hat{B}\theta_{\star} - \theta^{\mathsf{T}}\hat{B}\theta\right)}{(\theta_{\star}^{\mathsf{T}}\hat{B}\theta_{\star})(\theta^{\mathsf{T}}\hat{B}\theta)} + \frac{1}{\theta_{\star}^{\mathsf{T}}\hat{B}\theta_{\star}}\left(\theta^{\mathsf{T}}\hat{\Sigma}\theta - \theta_{\star}^{\mathsf{T}}\hat{\Sigma}\theta_{\star}\right). \end{split}$$

Since $R_n(\cdot; \mathbf{Z})$ is invariant to rescaling, we can assume without any loss of generality that $\|\theta\|_2 = \|\theta_\star\|_2 = 1$. Therefore for \mathbf{Z} satisfying H2-(1),we have from Lemma 10

$$\left|\bar{\mathsf{R}}_{n}(\theta;\mathbf{Z})\right| \leq \left(2\left(\frac{\bar{\kappa}}{\underline{\kappa}}\right)^{2} + 2\left(\frac{\bar{\kappa}}{\underline{\kappa}}\right)\right) \|\theta\theta^{\mathrm{T}} - \theta_{\star}\theta_{\star}^{\mathrm{T}}\|_{\mathsf{F}} \leq 4\left(\frac{\bar{\kappa}}{\underline{\kappa}}\right)^{2} \|\theta\theta^{\mathrm{T}} - \theta_{\star}\theta_{\star}^{\mathrm{T}}\|_{\mathsf{F}}. \quad (28)$$

It follows from the above observations that for \mathbf{Z} satisfying H2 the left hand side of (27) is bounded from below by

$$\left(\frac{1}{p^{\mathsf{u}}}\sqrt{\frac{\rho_{1}}{2\pi}}\right)^{s_{\star}} \int_{\mathbb{R}^{s_{\star}}} \exp\left(-\frac{\rho_{1}}{2}\|u\|_{2}^{2} - \frac{C}{2}n\|uu^{\mathsf{T}} - \theta_{\star}\theta_{\star}^{\mathsf{T}}\|_{\mathsf{F}}\right) du$$

$$\geq \left(\frac{1}{p^{\mathsf{u}}}\sqrt{\frac{\rho_{1}}{2\pi}}\right)^{s_{\star}} e^{-C\eta^{2}n} \int_{\mathcal{S}_{0}} e^{-\frac{\rho_{1}}{2}\|u\|_{2}^{2}} du,$$

where $C = 8(\bar{\kappa}/\underline{\kappa})^2$, $\eta \in (0,1)$ and $S_0 \stackrel{\text{def}}{=} \{u \in \mathbb{R}^{s_\star} : ||uu^{\mathrm{T}} - \theta_\star \theta_\star^{\mathrm{T}}||_{\mathsf{F}} \leq 2\eta^2\}$. Note that the integral $\int_{S_0} e^{-\frac{\rho_1}{2}||u||_2^2} \mathrm{d}u$ is invariant to change of variables by orthogonal matrices. Hence in that integral we can replace θ_\star by the unit vector $e = (0, \dots, 0, 1) \in \mathbb{R}^{s_\star}$. Using this and switching to polar coordinates, we write the integral as

$$\int_{\mathcal{S}_0} e^{-\frac{\rho_1}{2} \|u\|_2^2} du = \int_0^{+\infty} e^{-\frac{\rho_1}{2}r^2} r^{s_{\star}-1} dr \times \nu \left(\theta \in \mathcal{S}^{s_{\star}-1} : |\sin(\theta)| \le \eta \right),$$

where ν is the surface measure on the unit sphere $\mathcal{S}^{s_{\star}-1} = \{u \in \mathbb{R}^{s_{\star}} : ||u||_{2} = 1\}$, and $\sin(\theta)$ is the sine of the angle between θ and e. The measure ν ($\theta \in \mathcal{S}^{s_{\star}-1} : |\sin(\theta)| \leq \eta$) is equal to twice the spherical cap around the pole e defined by η . We use the formula of the spherical cap from ([21]) to write

$$\nu\left(\theta \in \mathcal{S}^{s_{\star}-1}: |\sin(\theta)| \leq \eta\right) = \frac{4\pi^{\frac{s_{\star}-1}{2}}}{\Gamma\left(\frac{s_{\star}-1}{2}\right)} \int_{0}^{\arcsin(\eta)} \sin^{s_{\star}-2}(\theta) d\theta$$
$$= \frac{4\pi^{\frac{s_{\star}-1}{2}}}{\Gamma\left(\frac{s_{\star}-1}{2}\right)} \int_{0}^{\eta} \frac{x^{s_{\star}-2}}{\sqrt{1-x^{2}}} dx \geq \frac{4\pi^{\frac{s_{\star}-1}{2}}}{\Gamma\left(\frac{s_{\star}-1}{2}\right)} \frac{\eta^{s_{\star}-1}}{s_{\star}-1}.$$

Whereas,

$$\int_0^{+\infty} e^{-\frac{\rho_1}{2}r^2} r^{s_{\star}-1} \mathrm{d}r = \frac{1}{2} \left(\frac{2}{\rho_1}\right)^{\frac{s_{\star}}{2}} \Gamma\left(\frac{s_{\star}}{2}\right).$$

It follows that

$$\int_{\mathcal{S}_0} e^{-\frac{\rho_1}{2} ||u||_2^2} du \ge \frac{2}{s_* \sqrt{\pi}} \left(\frac{2\pi}{\rho_1}\right)^{\frac{s_*}{2}} \eta^{s_* - 1}.$$

We conclude that for **Z** satisfying H2, and any $\eta \in (0,1)$, the left hand side of (27) is bounded from below by

$$\frac{2}{\sqrt{\pi} s_{\star}} \left(\frac{1}{p^{\mathsf{u}}} \right)^{s_{\star}} e^{-(s_{\star}-1) \log(1/\eta)} e^{-C\eta^{2} n} \geq e^{-(\mathsf{u}+1)(1+s_{\star}) \log(p \vee Cn)},$$

by taking $\eta = 1/\sqrt{Cn}$, and assuming that $p^{\mathsf{u}} \geq e^1 s_{\star}$. This concludes the proof.

We make use of the following version of the Davis-Kahan $\sin \Theta$ theorem taken from [39] Lemma 4.2.

Lemma 9. Let A be a $p \times p$ symmetric semipositive definite matrix and suppose that its eigenvalues satisfies $\lambda_1(A) > \lambda_2(A) \geq \ldots \geq \lambda_p(A)$. If a unit vector u is an eigenvector of A associated to the largest eigenvalue $\lambda_1(A)$, for all $v \in \mathbb{R}^p$, $||v||_2 = 1$ it holds

$$\langle A, uu' - vv' \rangle \ge \frac{1}{2} \left(\lambda_1(A) - \lambda_2(A) \right) \|uu' - vv'\|_F^2$$

We will need the following technical result.

Lemma 10. For any unit vectors u, v and square matrix B with matching dimensions, we have

$$|\langle B, uu^{\mathsf{T}} - vv^{\mathsf{T}} \rangle| \le 2||B||_{\mathsf{op}}||uu^{\mathsf{T}} - vv^{\mathsf{T}}||_{\mathsf{F}},\tag{29}$$

Proof. Indeed, we have

$$|\langle B, uu^{\mathrm{T}} - vv^{\mathrm{T}} \rangle| = |(u - v)^{\mathrm{T}}Bu + v^{\mathrm{T}}B(u - v)| \le 2||B||_{\mathsf{op}}||u - v||_{2}.$$

Similarly, we have $|\langle B, uu^{\mathrm{T}} - vv^{\mathrm{T}} \rangle| \leq 2||B||_{\mathsf{op}}||u + v||_2$. Hence

$$|\langle B, uu^{\mathrm{T}} - vv^{\mathrm{T}} \rangle| \le 2\|B\|_{\mathsf{op}} \min (\|u - v\|_2, \|u + v\|_2).$$

The result follows by noting that

$$||uu^{\mathrm{T}} - vv^{\mathrm{T}}||_{\mathsf{F}} > \min(||u - v||_{2}, ||u + v||_{2}).$$
 (30)

To see this, note that $||uu^{\mathrm{T}} - vv^{\mathrm{T}}||_{\mathsf{F}} = ||u - v||_2 ||u + v||_2 / \sqrt{2} = ||u - v||_2 \sqrt{2 - ||u - v||_2^2 / 2}$. Hence, if $||u - v||_2^2 \le 2$, then we have $||uu^{\mathrm{T}} - vv^{\mathrm{T}}||_{\mathsf{F}} \ge ||u - v||_2$. But if $||u - v||_2^2 > 2$ then $||uu^{\mathrm{T}} - vv^{\mathrm{T}}||_{\mathsf{F}} > ||u + v||_2$. Hence the result.

The next result describes the behavior of the Rayleigh quotient function that yields the posterior contraction result.

Lemma 11. Assume H2. For any $\theta \in \mathbb{R}^p$ such that $\|\theta\|_0 \leq s$, we have

$$R_n(\theta; \mathbf{Z}) - R_n(\theta_{\star}; \mathbf{Z}) \le -\frac{\mathsf{gap}}{2} \left(\frac{\kappa}{\kappa}\right)^2 \|\theta\theta^{\mathrm{T}} - \theta_{\star}\theta_{\star}^{\mathrm{T}}\|_F^2 + c_0 r_1 \|\theta\theta^{\mathrm{T}} - \theta_{\star}\theta_{\star}^{\mathrm{T}}\|_F.$$
(31)

Proof. Fix $\theta \in \mathbb{R}^p$ such that $\|\theta\|_0 \leq s$. Since the Rayleigh quotient is invariant under rescaling we can assume without any loss of generality that $\|\theta\|_2 = 1$. We have

$$\bar{\mathsf{R}}_{n}(\theta; \mathbf{Z}) = \mathsf{R}_{n}(\theta; \mathbf{Z}) - \mathsf{R}_{n}(\theta_{\star}; \mathbf{Z}) = \frac{\theta^{\mathsf{T}} \hat{\Sigma} \theta}{\theta^{\mathsf{T}} \hat{B} \theta} - \frac{\theta_{\star}^{\mathsf{T}} \hat{\Sigma} \theta_{\star}}{\theta_{\star}^{\mathsf{T}} \hat{B} \theta_{\star}} = \frac{\theta^{\mathsf{T}} \Sigma \theta}{\theta^{\mathsf{T}} B \theta} - \frac{\theta_{\star}^{\mathsf{T}} \Sigma \theta_{\star}}{\theta_{\star}^{\mathsf{T}} B \theta_{\star}} + \left\langle \hat{\Sigma} - \Sigma, \frac{\theta \theta^{\mathsf{T}}}{\theta^{\mathsf{T}} B \theta} - \frac{\theta_{\star} \theta_{\star}^{\mathsf{T}}}{\theta_{\star}^{\mathsf{T}} B \theta_{\star}} \right\rangle + \left\langle \hat{\Sigma}, \left[\frac{\theta \theta^{\mathsf{T}}}{\theta^{\mathsf{T}} \hat{B} \theta} - \frac{\theta \theta^{\mathsf{T}}}{\theta^{\mathsf{T}} B \theta} \right] - \left[\frac{\theta_{\star} \theta_{\star}^{\mathsf{T}}}{\theta_{\star}^{\mathsf{T}} \hat{B} \theta_{\star}} - \frac{\theta_{\star} \theta_{\star}^{\mathsf{T}}}{\theta_{\star}^{\mathsf{T}} B \theta_{\star}} \right] \right\rangle. \tag{32}$$

Set $S \stackrel{\text{def}}{=} B^{-1/2} \Sigma B^{-1/2}$, $w = B^{1/2} \theta / \|B^{1/2} \theta\|_2$, $w_{\star} = B^{1/2} \theta_{\star} / \|B^{1/2} \theta_{\star}\|_2$, and note that w_{\star} is an eigenvector of S associated to the largest eigenvalue of S. Hence by the curvature lemma (Lemma 9) we have

$$\frac{\theta^{\mathrm{T}} \Sigma \theta}{\theta^{\mathrm{T}} B \theta} - \frac{\theta_{\star}^{\mathrm{T}} \Sigma \theta_{\star}}{\theta_{\star}^{\mathrm{T}} B \theta_{\star}} = \langle S, ww^{\mathrm{T}} - w_{\star} w_{\star}^{\mathrm{T}} \rangle \leq -\frac{\mathsf{gap}}{2} \|ww^{\mathrm{T}} - w_{\star} w_{\star}^{\mathrm{T}}\|_{\mathsf{F}}^{2}.$$

Let $I \subseteq \{1, \ldots, p\}$ be the joint support of θ and θ_{\star} (hence $||I||_0 \leq s + s_{\star}$). Then we can express

$$\|ww^{\mathrm{T}} - w_{\star}w_{\star}^{\mathrm{T}}\|_{\mathsf{F}} = \left\| (B_{\mathsf{I},\mathsf{I}})^{1/2} \left(\frac{\theta_{\mathsf{I}}\theta_{\mathsf{I}}^{\mathrm{T}}}{\theta_{\mathsf{I}}^{\mathrm{T}}(B_{\mathsf{I},I})\theta_{\mathsf{I}}} - \frac{\theta_{\star\mathsf{I}}\theta_{\star\mathsf{I}}^{\mathrm{T}}}{\theta_{\star\mathsf{I}}^{\mathrm{T}}(B_{\mathsf{I},\mathsf{I}})\theta_{\star\mathsf{I}}} \right) (B_{\mathsf{I},\mathsf{I}})^{1/2} \right\|_{\mathsf{F}}.$$

We recall that for any square matrix A and invertible matrix B,

$$\|A\|_{\mathsf{F}} = \|B^{-1/2}B^{1/2}AB^{1/2}B^{-1/2}\|_{\mathsf{F}} \leq \|B^{-1/2}\|_{\mathsf{op}}^2 \|B^{1/2}AB^{1/2}\|_{\mathsf{F}},$$

where $||M||_{op}$ denotes the operator norm of M. With these observations in mind, we get

$$\|ww^{\mathrm{T}} - w_{\star}w_{\star}^{\mathrm{T}}\|_{\mathsf{F}} \geq \frac{1}{\|(B_{\mathsf{I},\mathsf{I}})^{-1/2}\|_{\mathsf{op}}^{2}} \left\| \frac{\theta_{\mathsf{I}}\theta_{\mathsf{I}}^{\mathrm{T}}}{\theta_{\mathsf{I}}^{\mathrm{T}}(B_{\mathsf{I},\mathsf{I}})\theta_{\mathsf{I}}} - \frac{\theta_{\star\mathsf{I}}\theta_{\star\mathsf{I}}^{\mathrm{T}}}{\theta_{\star\mathsf{I}}^{\mathrm{T}}(B_{\mathsf{I},\mathsf{I}})\theta_{\star\mathsf{I}}} \right\|_{\mathsf{F}}$$

$$\geq \underline{\kappa} \left\| \frac{\theta_{\mathsf{I}}\theta_{\mathsf{I}}^{\mathrm{T}}}{\theta_{\mathsf{I}}^{\mathrm{T}}(B_{\mathsf{I},\mathsf{I}})\theta_{\mathsf{I}}} - \frac{\theta_{\star\mathsf{I}}\theta_{\star\mathsf{I}}^{\mathrm{T}}}{\theta_{\star\mathsf{I}}^{\mathrm{T}}(B_{\mathsf{I},\mathsf{I}})\theta_{\mathsf{I}}} - \frac{\theta_{\star\mathsf{I}}\theta_{\star\mathsf{I}}^{\mathrm{T}}}{\theta_{\star\mathsf{I}}^{\mathrm{T}}(B_{\mathsf{I},\mathsf{I}})\theta_{\mathsf{I}}} \right\|_{\mathsf{F}}.$$

We note also that for any unit vectors u, v and symmetric invertible matrix B with matching dimension,

$$\left\| \frac{uu^{\mathsf{T}}}{u^{\mathsf{T}}Bu} - \frac{vv^{\mathsf{T}}}{v^{\mathsf{T}}Bv} \right\|_{\mathsf{F}}^{2} = \frac{(u^{\mathsf{T}}Bu - v^{\mathsf{T}}Bv)^{2}}{(u^{\mathsf{T}}Bu)^{2}(v^{\mathsf{T}}Bv)^{2}} + \frac{\|uu^{\mathsf{T}} - vv^{\mathsf{T}}\|_{\mathsf{F}}^{2}}{(u^{\mathsf{T}}Bu)(v^{\mathsf{T}}Bv)} \ge \frac{\|uu^{\mathsf{T}} - vv^{\mathsf{T}}\|_{\mathsf{F}}^{2}}{(u^{\mathsf{T}}Bu)(v^{\mathsf{T}}Bv)}. \tag{33}$$

Hence, under H2,

$$\|ww^{\scriptscriptstyle \mathrm{T}} - w_{\star}w_{\star}^{\scriptscriptstyle \mathrm{T}}\|_{\mathsf{F}}^2 \geq \left(\frac{\underline{\kappa}}{\bar{\kappa}}\right)^2 \|\theta_{\mathsf{I}}\theta_{\mathsf{I}}^{\scriptscriptstyle \mathrm{T}} - \theta_{\star\mathsf{I}}\theta_{\star\mathsf{I}}^{\scriptscriptstyle \mathrm{T}}\|_{\mathsf{F}}^2 = \left(\frac{\underline{\kappa}}{\bar{\kappa}}\right)^2 \|\theta\theta^{\scriptscriptstyle \mathrm{T}} - \theta_{\star}\theta_{\star}^{\scriptscriptstyle \mathrm{T}}\|_{\mathsf{F}}^2$$

In conclusion we have

$$\frac{\theta^{\mathrm{T}} \Sigma \theta}{\theta^{\mathrm{T}} B \theta} - \frac{\theta_{\star}^{\mathrm{T}} \Sigma \theta_{\star}}{\theta^{\mathrm{T}} B \theta_{\star}} \leq -\frac{\mathsf{gap}}{2} \left(\frac{\underline{\kappa}}{\bar{\kappa}}\right)^{2} \|\theta \theta^{\mathrm{T}} - \theta_{\star} \theta_{\star}^{\mathrm{T}}\|_{\mathsf{F}}^{2}. \tag{34}$$

The second term from (32) can be written as

$$\begin{split} \left| \left\langle \hat{\Sigma} - \Sigma, \frac{\theta \theta^{\mathrm{T}}}{\theta^{\mathrm{T}} B \theta} - \frac{\theta_{\star} \theta_{\star}^{\mathrm{T}}}{\theta_{\star}^{\mathrm{T}} B \theta_{\star}} \right\rangle \right| &= \left| \left\langle (\hat{\Sigma})_{\mathsf{I},\mathsf{I}} - \Sigma_{\mathsf{I},\mathsf{I}}, \frac{\frac{\theta_{\mathsf{I}} \theta_{\mathsf{T}}^{\mathrm{T}}}{\theta^{\mathrm{T}} B \theta} - \frac{\theta_{\star} \theta_{\star}^{\mathrm{T}}}{\theta_{\star}^{\mathrm{T}} B \theta_{\star}}}{\left\| \frac{\theta_{\mathsf{I}} \theta_{\mathsf{T}}^{\mathrm{T}}}{\theta^{\mathrm{T}} B \theta} - \frac{\theta_{\star} \theta_{\star}^{\mathrm{T}}}{\theta_{\star}^{\mathrm{T}} B \theta_{\star}} \right\|_{\mathsf{F}}} \right\rangle \right| \left\| \frac{\theta_{\mathsf{I}} \theta_{\mathsf{I}}^{\mathrm{T}}}{\theta^{\mathrm{T}} B \theta} - \frac{\theta_{\star} \theta_{\star}^{\mathrm{T}}}{\theta_{\star}^{\mathrm{T}} B \theta_{\star}} \right\|_{\mathsf{F}} \\ &\leq \max_{M \in \mathbb{R}^{\mathsf{I} \times \mathsf{I}} : \ \|M\|_{\mathsf{F}} = 1, \ \mathsf{Rank}(M) \leq 2} \ \left| \left\langle (\hat{\Sigma})_{\mathsf{I},\mathsf{I}} - \Sigma_{\mathsf{I},\mathsf{I}}, M \right\rangle \right| \times \left\| \frac{\theta_{\mathsf{I}} \theta_{\mathsf{I}}^{\mathrm{T}}}{\theta^{\mathrm{T}} B \theta} - \frac{\theta_{\star} \theta_{\star}^{\mathrm{T}}}{\theta_{\star}^{\mathrm{T}} B \theta_{\star}} \right\|_{\mathsf{F}}. \end{split}$$

And we note from (33) and Lemma 10 that for **Z** satisfying H2.

$$\left\| \frac{\theta_{\mathsf{I}}\theta_{\mathsf{I}}^{\mathsf{T}}}{\theta^{\mathsf{T}}B\theta} - \frac{\theta_{\star\mathsf{I}}\theta_{\star\mathsf{I}}^{\mathsf{T}}}{\theta_{\star}^{\mathsf{T}}B\theta_{\star}} \right\|_{\mathsf{F}}^{2} \leq \frac{1}{\underline{\kappa}^{4}} \left\langle B_{\mathsf{I}\mathsf{I}}, \theta_{\mathsf{I}}\theta_{\mathsf{I}}^{T} - \theta_{\star,\mathsf{I}}\theta_{\star,\mathsf{I}}^{\mathsf{T}} \right\rangle^{2} + \frac{1}{\underline{\kappa}^{2}} \left\| \theta_{\mathsf{I}}\theta_{\mathsf{I}}^{T} - \theta_{\star,\mathsf{I}}\theta_{\star,\mathsf{I}}^{\mathsf{T}} \right\|_{\mathsf{F}}^{2}$$

$$\leq \frac{1}{\underline{\kappa}^{2}} \left(1 + 2 \left(\frac{\bar{\kappa}}{\underline{\kappa}} \right)^{2} \right) \|\theta\theta^{T} - \theta_{\star}\theta_{\star}^{\mathsf{T}}\|_{\mathsf{F}}^{2}. \tag{35}$$

Therefore for **Z** satisfying H2,

$$\left| \left\langle \hat{\Sigma} - \Sigma, \frac{\theta \theta^{\mathrm{T}}}{\theta^{\mathrm{T}} B \theta} - \frac{\theta_{\star} \theta_{\star}^{\mathrm{T}}}{\theta_{\star}^{\mathrm{T}} B \theta_{\star}} \right\rangle \right| \leq c_0 \mathsf{r}_1 \|\theta \theta^T - \theta_{\star} \theta_{\star}^{\mathrm{T}}\|_{\mathsf{F}}. \tag{36}$$

We process the last term in (32) as follows.

$$\left\langle \hat{\Sigma}, \left[\frac{\theta \theta^{\mathrm{T}}}{\theta^{\mathrm{T}} \hat{B} \hat{\theta}} - \frac{\theta \theta^{\mathrm{T}}}{\theta^{\mathrm{T}} B \hat{\theta}} \right] - \left[\frac{\theta_{\star} \theta_{\star}^{\mathrm{T}}}{\theta_{\star}^{\mathrm{T}} \hat{B} \theta_{\star}} - \frac{\theta_{\star} \theta_{\star}^{\mathrm{T}}}{\theta_{\star}^{\mathrm{T}} B \theta_{\star}} \right] \right\rangle \\
= \frac{\theta^{\mathrm{T}} \hat{\Sigma} \hat{\theta}}{\theta^{\mathrm{T}} \hat{B} \hat{\theta}} \left\langle B - \hat{B}, \frac{\theta \theta^{\mathrm{T}}}{\theta^{\mathrm{T}} B \hat{\theta}} \right\rangle - \frac{\theta_{\star}^{\mathrm{T}} \hat{\Sigma} \theta_{\star}}{\theta_{\star}^{\mathrm{T}} \hat{B} \theta_{\star}} \left\langle B - \hat{B}, \frac{\theta_{\star} \theta_{\star}^{\mathrm{T}}}{\theta_{\star}^{\mathrm{T}} B \theta_{\star}} \right\rangle \\
= \left(\frac{\theta^{\mathrm{T}} \hat{\Sigma} \hat{\theta}}{\theta^{\mathrm{T}} \hat{B} \hat{\theta}} - \frac{\theta_{\star}^{\mathrm{T}} \hat{\Sigma} \hat{\theta}_{\star}}{\theta_{\star}^{\mathrm{T}} \hat{B} \hat{\theta}_{\star}} \right) \left\langle B - \hat{B}, \frac{\theta \theta^{\mathrm{T}}}{\theta^{\mathrm{T}} B \hat{\theta}} \right\rangle + \frac{\theta_{\star}^{\mathrm{T}} \hat{\Sigma} \theta_{\star}}{\theta_{\star}^{\mathrm{T}} \hat{B} \hat{\theta}_{\star}} \left\langle B - \hat{B}, \frac{\theta \theta^{\mathrm{T}}}{\theta^{\mathrm{T}} B \hat{\theta}} - \frac{\theta_{\star} \theta_{\star}^{\mathrm{T}}}{\theta_{\star}^{\mathrm{T}} B \hat{\theta}_{\star}} \right\rangle. \tag{37}$$

Hence for **Z** satisfying H2, the first term in the last display can be bounded, similar to (28), as

$$\begin{split} \left| \left(\frac{\theta^{\mathrm{T}} \hat{\Sigma} \theta}{\theta^{\mathrm{T}} \hat{B} \theta} - \frac{\theta_{\star}^{\mathrm{T}} \hat{\Sigma} \theta_{\star}}{\theta_{\star}^{\mathrm{T}} \hat{B} \theta_{\star}} \right) \left\langle B - \hat{B}, \frac{\theta \theta^{\mathrm{T}}}{\theta^{\mathrm{T}} B \theta} \right\rangle \right| \\ & \leq \frac{1}{\underline{\kappa}} \lambda_{\mathsf{max}} (\hat{B} - B, s) \left[4 \left(\frac{\overline{\kappa}}{\underline{\kappa}} \right)^{2} \|\theta \theta^{\mathrm{T}} - \theta_{\star} \theta_{\star}^{\mathrm{T}}\|_{\mathsf{F}} \right] \\ & \leq \frac{4}{\underline{\kappa}} \lambda_{\mathsf{max}} (\hat{B} - B, s) \left(\frac{\overline{\kappa}}{\underline{\kappa}} \right)^{2} \|\theta \theta^{\mathrm{T}} - \theta_{\star} \theta_{\star}^{\mathrm{T}}\|_{\mathsf{F}}. \end{split}$$

The rightmost of (37) is similar to (36):

$$\left| \frac{\theta_{\star}^{\mathrm{T}} \hat{\Sigma} \theta_{\star}}{\theta_{\star}^{\mathrm{T}} \hat{B} \theta_{\star}} \left\langle B - \hat{B}, \frac{\theta \theta^{\mathrm{T}}}{\theta^{\mathrm{T}} B \theta} - \frac{\theta_{\star} \theta_{\star}^{\mathrm{T}}}{\theta_{\star}^{\mathrm{T}} B \theta_{\star}} \right\rangle \right| \leq c_{0} \mathsf{r}_{1} \|\theta \theta^{T} - \theta_{\star} \theta_{\star}^{\mathrm{T}}\|_{\mathsf{F}}.$$

In conclusion the last term in (32) is bounded from above by

$$\left| \left\langle \hat{\Sigma}, \left[\frac{\theta \theta^{\mathrm{T}}}{\theta^{\mathrm{T}} \hat{B} \theta} - \frac{\theta \theta^{\mathrm{T}}}{\theta^{\mathrm{T}} B \theta} \right] - \left[\frac{\theta_{\star} \theta_{\star}^{\mathrm{T}}}{\theta_{\star}^{\mathrm{T}} \hat{B} \theta_{\star}} - \frac{\theta_{\star} \theta_{\star}^{\mathrm{T}}}{\theta_{\star}^{\mathrm{T}} B \theta_{\star}} \right] \right\rangle \right| \leq c_{0} \mathsf{r}_{1} \|\theta \theta^{T} - \theta_{\star} \theta_{\star}^{\mathrm{T}}\|_{\mathsf{F}}. \tag{38}$$

We conclude from (34-38) that for **Z** satisfying H2

$$\mathsf{R}_n(\boldsymbol{\theta}; \mathbf{Z}) - \mathsf{R}_n(\boldsymbol{\theta}_\star; \mathbf{Z}) \leq -\frac{\mathsf{gap}}{2} \left(\frac{\underline{\kappa}}{\bar{\kappa}}\right)^2 \|\boldsymbol{\theta}\boldsymbol{\theta}^{\scriptscriptstyle \mathrm{T}} - \boldsymbol{\theta}_\star \boldsymbol{\theta}_\star^{\scriptscriptstyle \mathrm{T}}\|_{\mathsf{F}}^2 + c_0 \mathsf{r}_1 \|\boldsymbol{\theta}\boldsymbol{\theta}^T - \boldsymbol{\theta}_\star \boldsymbol{\theta}_\star^{\scriptscriptstyle \mathrm{T}}\|_{\mathsf{F}}.$$

This ends the proof.

B Description of the coupled chain for mixing time estimation

Here we introduce the specific coupled chain that we employ. We refer the reader to [7] and [19] for more details on the construction of such coupled kernels. The striking point of their method is that even in problems as involved in the one considered in this work, these coupled kernels are easy to construct and simulate.

We modify Algorithm 1 to construct the coupled kernel \check{P} . Let $(\delta^{(1,t)}, \theta^{(1,t)}, k^{(1,t)})$ and let $(\delta^{(2,t)}, \theta^{(2,t)}, k^{(2,t)})$ denote the states of the two chains at time t. At some iteration $t \geq 1$, given

 $(\delta^{(1,L+t)}, \theta^{(1,L+t)}, k^{(1,L+t)}) = (\delta^{(1)}, \theta^{(1)}, k^{(1)})$ and $(\delta^{(2,t)}, \theta^{(2,t)}, k^{(2,t)}) = (\delta^{(2)}, \theta^{(2)}, k^{(2)})$, we now describe how to generate the next state of the coupled chain.

In step 1, to update $\delta^{(1)}$ and $\delta^{(2)}$, we first make use of the same randomly drawn subset J. For i=1,2, drawing $\bar{\delta}^{(i)} \sim Q_{k,\theta}^{(J)}(\delta^{(i)},\cdot)$ is equivalent to let $\bar{\delta}_{-J}^{(i)} = \delta_{-J}^{(i)}$, and for any $j \in J$, draw $\bar{\delta}_j^{(i)} \sim \mathbf{Ber}(q_j^{(i)})$ which we implement in the following way. We first draw a common uniform number $u_j \sim \mathbf{Uniform}(0,1)$, then we obtain $\bar{\delta}_j^{(i)} = \mathbf{1}\{q_j^{(i)} \leq u_j\}$ for i=1,2.

In step 2, to update $\theta^{(1)}$ and $\theta^{(2)}$, we partition the indices $\{1,\ldots,p\}$ into four groups: $G_{ab}=\{j:\bar{\delta}_j^{(1)}=a,\bar{\delta}_j^{(2)}=b\}$ for a,b=0,1. To update the components of $\theta_{G_{00}}^{(1)}$ and $\theta_{G_{00}}^{(2)}$, for any $j\in G_{00}$ we first draw a common standard normal random variables Z_j , and then obtain $\bar{\theta}_j^{(i)}=t_{k^{(i)}}\rho_0^{-1}Z_j$ for i=1,2. To update the components of $\theta_{G_{01}}^{(1)}$ and $\theta_{G_{01}}^{(2)}$, for any $j\in G_{01}$ we again first draw a common standard normal random variables Z_j , and then obtain $\bar{\theta}_j^{(1)}=t_{k^{(1)}}\rho_0^{-1}Z_j$, and simultaneously draw $\bar{\theta}_j^{(2)}$ using MALA with proposal $\theta_j^{(2)}+\eta_{k^{(2)}}\nabla\log\pi(\theta_j^{(2)})+\sqrt{2\eta_{k^{(2)}}}Z_j$, where $\pi(\theta_j^{(2)})$ is the marginal posterior distribution of $\theta_j^{(2)}$. Notice that the joint distribution of $[\theta^{(2)}]_{\bar{\delta}^{(2)}}$ is given by $W_{k^{(2)},\bar{\delta}^{(2)}}$, whose density is proportional to (18). A similar update procedure is used for updating the components of $\theta_{G_{10}}^{(1)}$ and $\theta_{G_{10}}^{(2)}$. To update the components of $\theta_{G_{11}}^{(1)}$ and $\theta_{G_{11}}^{(2)}$, we draw reflection-coupled MALA proposals in [7], and then for the acceptance step, $\theta_{G_{11}}^{(1)}$ and $\theta_{G_{11}}^{(2)}$ share the same uniform random variables.

In step 3, to update $k^{(1)}$ and $k^{(2)}$, we first draw two common uniform numbers $w, u \sim \mathbf{Uniform}(0,1)$ to couple two chains in the Metropolis-Hastings algorithm approach. In the random walk proposal step, if $w \leq 0.5$, for both two chains we propose the left neighbor except at the boundaries. In the acceptance step, for both chains, we accept the proposal if the acceptance probability is greater than u, otherwise we reject the proposal.

C An adaptive version of simulated tempering for Canonical correlation analysis

Algorithm 2 Adaptive version of simulated tempering for Canonical correlation analysis

Model Input: Matrices \hat{A}, \hat{B} , prior parameters ρ_0, ρ_1, q .

MCMC Input: Number of iterations N, Batch size J, temperatures $1 = t_1 < \dots, < t_K$.

Adaptive MCMC Input: a = 10 and $w \in (0, 1)$.

MCMC Initialization: Set $k^{(0)} = 1$. Draw $\delta_j^{(0)} \stackrel{i.i.d.}{\sim} \mathbf{Ber}(0.5), \forall j = 1, \dots, p$, and independently $\theta^{(0)} \sim \mathbf{N}(0, I_p)$.

Adaptation Parameters Initialization : . Set $\tau^{(0)} = \mathbf{0} \in \mathbb{R}^K$, $v^{(0)} = (0, \dots, 0) \in \mathbb{R}^K$, and choose $c^{(0)} \in (0, \infty)^K$.

for t = 1 to N - 1, given $(k^{(t)}, \delta^{(t)}, \theta^{(t)}) = (k, \delta, \theta), \ \tau^{(t)} = \tau, \ c^{(t)} = c, \ \text{and} \ v^{(t)} = v \ \mathbf{do}$

- 1. **Update** δ : Uniformly randomly select a subset J from $\{1, \ldots, p\}$ of size J without replacement, and draw $\bar{\delta} \sim Q_{k,\theta}^{(\mathsf{J})}(\delta,\cdot)$, where the transition kernel described in (17).
- 2. Update θ and τ : Draw the components of $[\bar{\theta}]_{\bar{\delta}^c}$ independently from $\mathbf{N}(0, \rho_0^{-1}t_k)$. Draw $[\bar{\theta}]_{\bar{\delta}} \sim P_{\eta,k,\bar{\delta}}([\theta]_{\bar{\delta}},\cdot)$, where $\eta = e^{\tau_k}$ and $P_{\eta,k,\bar{\delta}}$ denotes the transition kernel of the MALA with step-size η and invariant distribution given by $W_{k,\bar{\delta}}$, whose density is proportional to (18). Denote the acceptance probability of the MALA update. Set

$$\bar{\tau}_k = \tau_k + v_k^{-0.6} (\alpha - 0.3),$$

and for $i \neq k$, set $\bar{\tau}_i = \tau_i$.

3. **Update** k, c and v: Draw $\bar{k} \sim T_{\bar{\delta},\bar{\theta}}(k,\cdot)$, where $T_{\delta,\theta}$ is the transition kernel of the Metropolis-Hastings on $\{1,\ldots,K\}$ with invariant distribution given by (19) and random walk proposal that has reflection at the boundaries. We then set

$$\bar{c}_{\bar{k}} = c_{\bar{k}}e^a, \quad \bar{v}_{\bar{k}} = v_{\bar{k}} + 1,$$

and for $i \neq \bar{k}$, $\bar{c}_i = c_i$, and $\bar{v}_i = v_i$.

- 4. Update a and v: If $\|\bar{v}/(\sum_{k=1}^K \bar{v}_k) 1/K\|_{\infty} \le w/K$, then set $a = a/2, \bar{v} = \mathbf{0} \in \mathbb{R}^K$.
- 5. New MCMC state: Set $(\delta^{(t+1)}, \theta^{(t+1)}, k^{(t+1)}) = (\bar{\delta}, \bar{\theta}, \bar{k}), \ \tau^{(t+1)} = \bar{\tau}, \ c^{(t+1)} = \bar{c}, \ \text{and} \ v^{(t+1)} = \bar{v}.$

end for

Output: $\{(\delta^{(t)}, \theta^{(t)}, k^{(t)}): 0 \le t \le N \text{ s.t. } k^{(t)} = 1\}$